



Modelling mussel (*Mytilus spp.*) microplastic accumulation.

Natalia Stamataki^{1,2,3}, Yannis Hatzonikolakis^{2,4}, Kostas Tsiaras², Catherine Tsangaris²,
George Petihakis³, Sarantis Sofianos¹, George Triantafyllou^{2,*}

¹Department of Environmental Physics, University of Athens, 15784 Athens, Greece

²Hellenic Centre for Marine Research (HCMR), Athens-Sounio Avenue, MavroLithari, 19013 Anavyssos, Greece

³Hellenic Centre for Marine Research (HCMR), 71003 Heraklion, Greece

⁴Department of Biology, University of Athens, 15784, Greece

*Corresponding author: gt@hcmr.gr

Abstract: Microplastics (MPs) are a contaminant of growing concern due to their widespread distribution and interactions with marine species, such as filter feeders. To investigate the MPs accumulation by wild and cultured mussels, a Dynamic Energy Budget (DEB) model was developed and validated with the available field data of *Mytilus edulis* (wild) from the North Sea and *Mytilus galloprovincialis* (cultured) from the Northern Ionian Sea. Towards a generic DEB model, the site-specific model parameter, half saturation coefficient (X_k) was applied as a power function of food density for the cultured mussel, while for the wild it was calibrated to a constant value. The DEB-accumulation model simulated the uptake and excretion rate of MPs, taking into account environmental characteristics (temperature and chlorophyll-a). An accumulation of MPs equal to 0.64 particles individual⁻¹ (fresh tissue mass 1.9 g) and 0.91 particles individual⁻¹ (fresh tissue mass 3.4 g) was found for the wild and cultured mussel respectively, in agreement with the field data. The inverse experiments investigating the depuration time of the wild and cultured mussel in a clean from MPs environment showed a 90% removal of MPs load after 3 and 14 days, respectively. Furthermore, sensitivity tests on model parameters and forcing functions highlighted that besides MPs concentration, the accumulation is highly depended on temperature and chlorophyll-a of the surrounding environment. For this reason, an empirical equation was found relating directly the concentration of MPs in seawater, with MPs accumulation in mussel's soft tissue, temperature and chlorophyll-a.





1. Introduction

Microplastic particles (MPs) are synthetic organic polymers with size below 5 mm (Arthur et al., 2009) that originate from a variety of sources including ~~mainly~~ those that are manufactured for particular household or industrial activities, such as facial scrubs, toothpastes and resin pellets used in the plastic industry (primary MPs), and those formed from the fragmentation of larger plastic items (secondary MPs) (GESAMP, 2015). Eriksen et al. (2014) estimated that more than 5 trillion microplastic particles, weighing over 250,000 tons, float in the oceans. Due to their composition, density and shape, MPs are highly persistent in the environment and are, therefore, accumulating in different marine compartments at increasing rates: surface and deeper layers in the water column, as well as at the seafloor and within the sediments (Moore et al., 2001, Lattin et al., 2004, Thompson, 2004, Lusher, 2015). Since the majority of MPs entering the marine environment, originate from the land (i.e. land-fills, littering of beaches and coastal areas, rivers, floodwaters, untreated municipal sewerage, industrial emissions), the threat of MPs pollution in the coastal zone puts considerable pressure on the coastal ecosystems (Cole et al., 2011, Andrady, 2011). In recent years, initiatives under various projects (i.e. CLAIM, DeFishGear) target at evaluating the threat and impact of marine litter pollution; the European framework of JERICO-RI focuses on a sustainable research infrastructure in the coastal area to support the monitoring, science and management of coastal marine areas (<http://www.jerico-ri.eu/>). In the framework of JERICO-NEXT, a recent study addressed the environmental threats and gaps in monitoring programmes in European coastal waters, including the marine litter (i.e. MPs) as one of the most commonly identified threat to the marine environment and highlighted the need for improved monitoring of the MPs distribution and their impacts in European coastal environments (Painting et al., 2019).

Numerous studies have revealed that MPs are ingested either directly or through lower trophic prey by animals ~~from~~ all levels of the food web; from zooplankton (Cole et al., 2013), small pelagic fishes and mussels (Digka et al., 2018a) to mesopelagic fishes (Wieczorek et al., 2018) and large predators like tuna and swordfish (Romeo et al., 2015). Microplastic ingestion by marine animals can potentially affect animal health and raises toxicity concerns, since plastics can facilitate the transfer of chemical additives and/or hydrophobic organic contaminants to biota (Mato et al., 2001, Rios et al., 2007, Teuten et al., 2007, 2009, Hirai et al., 2011). Human, as a top predator, is also contaminated by MPs (Schwabl et al., 2019). Mussel and small fishes that are commonly consumed whole, without removing digestive tracts, where MPs are concentrated, are among the most likely pathways for MPs to embed in the human diet (Smith et al., 2018). Especially regarding marine organisms (i.e. mussels), it is notable that the levels of their contamination has been added to the



European database (www.ecsafeseafooddbase.eu) as an environmental variable of growing concern, reflecting the health status (Marine Strategy Framework Directive (MSFD) Descriptor 10 – Marine Litter (Decision 2017/848/EU)) (De Witte et al., 2014, Vandermeersch et al., 2015, Digka et al., 2018a). Today, a series of studies have denoted the presence of MPs in mussels' tissue intended for human consumption (Van Cauwenberghe and Janssen, 2014, Mathalon and Hill, 2014, Li et al., 2016, 2018, Hantoro et al., 2019). For instance, in a recent study, Li et al. (2018) sampled mussels from coastal waters and supermarkets in the U.K and estimated that a plate of 100g mussels contains 70 MPs that will be ingested by the consumer. The presence of MPs in mussels has been also demonstrated during laboratory trials in their faeces, intestinal tract (Von Moos et al., 2012, Van Cauwenberghe et al., 2015, Wegner et al., 2012, Khan and Prezant, 2018), as well as in their circulatory system (Browne et al., 2008). Other laboratory studies showed several effects of microplastic ingestion in laboratory exposed mussels, including histological changes, inflammatory responses, immunological alterations, lysosomal membrane destabilization, reduced filtering activity, neurotoxic effects, oxidative stress effects, increase in hemocyte mortality, dysplasia, genotoxicity and transcriptional responses (reviewed by Li et al., 2019). However, the tested concentrations of MPs in laboratory experiments are frequently unrealistic, being several orders of magnitude higher (2 to 7 orders of magnitude) than the observed seawater concentrations (Van Cauwenberge et al., 2015, Lenz et al. 2016).

Mussels, through their extensive filtering activity, feed on planktonic organisms that have similar size with MPs (Browne et al., 2007) and considering also their inability to select particles with high energy value (i.e. phytoplankton) during filtration (Vahl, 1972, Saraiva et al., 2011a), they are directly exposed to MPs' contamination. Recent studies suggest a positive linear correlation between MPs concentration in mussels and surrounding waters (Capolupo et al., 2018, Qu et al. 2018, Li et al. 2019). The filtering activity of mussels, which directly affects the resulting MPs accumulation, is a complicated process that is controlled by other factors (food availability, temperature, tides etc.).

The purpose of the present work is to study the accumulation of MPs by the mussel and reveal relations between accumulated concentrations in mussels' soft parts and environmental features. In this context, an accumulation model was developed based on Dynamic Energy Budget theory (DEB, Kooijman, 2000) and applied in two different regions, in two different modes of life (wild and cultivated): in the North Sea (*M. edulis*, wild) and in the Northern Ionian Sea (*M. galloprovincialis*, cultivated). DEB theory provides all the necessary detail to model the feeding processes and aspects of the mussel metabolism, taking into account the impact of the environmental variability on the simulated individual. Apart from modeling the growth of bivalves (Rosland et al., 2009, Sara et al., 2012, Thomas et al., 2011, Saraiva et al., 2012, Hatzonikolakis et



al., 2017, Monaco & McQuaid, 2018), DEB models have been used to study other processes as well, such as bioaccumulation of PCBs (Polychlorinated Biphenyls) and POPs (Persistent Organic Compounds) (Zaldivar, 2008), trace metals (Casas and Bacher, 2006) and the impact of climate change on individual's physiology (Sara et al., 2014). However, to our knowledge this is the first time that a DEB-based model is used to assess the uptake and excretion rates of MPs in mussels.

2. Materials and Methods

2.1 Study areas and field data

The North Sea is a large semi-enclosed sea on the continental shelf of north-west Europe with a total surface area of 850,000 km² and is bounded by the coastlines of 9 countries. The sea is shallow (mean depth 90 m), getting deeper towards the north (up to 725 meters) and the semi-diurnal tide (tidal range 0-5 m) is the dominant feature of the region (Otto et al., 1990). Major rivers, such as Rhine, Elbe, Weser, Ems and Thames discharge into the southern part of the sea (Lacroix et al., 2004), making this area a productive ecosystem. In this study, the area is limited along the French, Belgian and Dutch North Sea coast (N 50.98°-51.46°, W 1.75°-3.54°). This is located close to harbors, where shipping, industrial and agricultural activity is high, putting considerable pressure on the ecological systems of the region (Van Cauwenberghe et al., 2015).

The MPs concentration in mussels' tissue and seawater that were used to validate and force the model respectively at its North Sea implementation were derived from Van Cauwenberghe et al. (2015). Van Cauwenberghe et al. (2015) examined the presence of MPs in wild mussels (*M. edulis*), and thus collected both biota and water at 6 sampling stations along the French, Belgian and Dutch North Sea coast in late summer of 2011. *M. edulis* (mean shell length: 4 ± 0.5 cm and wet weight (w.w.): 2 ± 0.7 g) and water samples were randomly collected on the local breakwaters, in order to assess the MPs concentration in the organisms and their habitat. MPs were present in all analyzed samples, both organisms and water. Seawater samples (N=12) had MPs (<1mm) on average 0.4 ± 0.3 particles L⁻¹ (range: 0.0 – 0.8 particles L⁻¹) and *M. edulis* contained on average 0.2 ± 0.3 particles g⁻¹w.w. (or 0.4 ± 0.3 particles individual⁻¹) (Van Cauwenberghe et al., 2015). The size range of MPs found within the mussels was 20-90 µm (size <1 mm).

The Northern Ionian Sea is located in the transition zone between the Adriatic and Ionian Sea. The long and complex coastline, presents a high diversity of hydrodynamic and sedimentary



features. Rivers discharging into the Northern Ionian Sea include Kalamas/Thyamis (Greece) and Butrinto (Albania) (Skoulikidis et al., 2009), making the area suitable for aquaculture. Small farming sites and shellfish grounds are operating in Thesprotia (northwestern Ionian Sea) (Theodorou et al., 2011). The main source of marine litter inputs in the area originates from anthropogenic activities that mainly include shoreline tourism and recreational activities, poor wastewater management, agricultural practices, fisheries, aquacultures and shipping (Vlachogianni et al., 2017; Digka et al., 2018a). According to Politikos et al. (2020), the area around the Corfu island (Northern Ionian Sea) is characterized as a retention area of litter particles probably due to the prevailing weak coastal circulation. Furthermore, a northward current on the east Ionian Sea facilitates the transfer of litter particles towards the Adriatic Sea, which has been characterized as a hotspot of marine litter and one of the most affected areas in the Mediterranean Sea (Pasquini et al., 2016, Vlachogianni et al., 2017, Liubartseva et al., 2018, Politikos et al., 2020).

The field data used to validate the model output in the N. Ionian Sea were obtained from Digka et al. (2018b, 2018a). In the framework of the “DeFishGear” project, mussels (*M. galloprovincialis*) were collected by hand from a long line type mussel culture farm in Thesprotia (N 39.606567° E 20.149421°), in summer 2015 (July) at a sampling depth up to 3 m (Digka et al., 2018a). The average MPs accumulation was calculated from a total population of 40 mussels originated from the farm, with 18 of them found contaminated with MPs (46.25%). The average load of MPs (size <1 mm) per mussel (mean shell length 5.0 ± 0.3 cm) was 0.9 ± 0.2 particles individual⁻¹ and the size of MPs found in the mussel’s tissue ranged from 55 to 620 µm. Both clean and contaminated mussels were included in the calculated mean value in order to represent the mean state of the contamination level for the individual inhabiting the study area.

The seawater concentration of MPs for the N. Ionian Sea implementation was obtained from Digka et al. (2018b) and the DeFishGear project results (<http://www.defishgear.net/project/main-lines-of-activities>). In total, 12 manta net tows were conducted in the region, collecting a total number of n1=2,027 particles on October 2014 and n2=1,332 on April 2015, leading to an average of 280 particles per tow with size <1 mm and >330 µm (Digka et al., 2018b). In order to estimate the mean MPs concentration in the region, expressed as particles per volume, the dimensions of the manta net (W 60 cm H 24 cm, rectangular frame opening, mesh size 330 µm) and the sampling distance of each tow (~2 km) were used by multiplying the sample surface of the net by the trawled distance in meters (Maes et al., 2017), which resulted in a mean MPs concentration of 1.17 particles m⁻³ (233,333 particles km⁻²). Moreover, in the wider region of the Adriatic Sea, Zeri et al. (2018) found a mean density of $315,009 \pm 568,578$ particles km⁻² (1.58 ± 2.84 particles m⁻³), out of which 34% sized <1 mm. A relatively high value of standard deviation (one order of magnitude higher than the mean value) is adopted (0.0012 ± 0.024 particles L⁻¹), considering that the mussel farm is



established in an enclosed gulf and close to the coast, since, according to Zeri et al. (2018), the abundance of MPs is one order of magnitude higher in inshore (<4 km) compared to offshore waters (>4 km). Furthermore, it may be assumed that the adopted range (standard deviation is also multiplied by a factor of 2) includes also the smaller particles sized between 50 μm and < 330 μm , which have been found in mussel's tissue (Digka et al., 2018a), but were overlooked during the seawater sampling due to the manta net's mesh size (> 330 μm). According to Enders et al. (2015) the relative abundance of small particles (50- 300 μm) compared to particles larger than 300 μm is approximately 50%.

2.2 DEB model description

In the present study, a Dynamic Energy Budget (DEB, Kooijman, 2000, 2010) model is used as basis to simulate the accumulation of MPs by mussels. In DEB theory (Kooijman, 2000), the energy assimilated through food by the simulated individual is stored in a reserve compartment from where a fixed energy fraction κ is allocated for growth and somatic maintenance, with a priority for maintenance. The remaining energy ($1 - \kappa$) is spent on maturity maintenance and reproduction. The individual's condition is defined by the dynamics of three state variables: energy reserves E (joules), structural volume V (cm^3) and energy allocated to reproduction R (joules). The energy flow through the organism is controlled by the fluctuations of the available food density and temperature characterizing the surrounding environment.

The DEB model implemented here is an extended version of the model described in Hatzonikolakis et al. (2017), where the growth of the Mediterranean mussel is simulated by taking into account only the assimilation rate of the individual. Since the present study focuses on simulating the MPs accumulation, it is crucial to include a detailed representation of the mussel's feeding mechanism. In this context, the DEB model was extended by including the clearance (C_r), filtration (\dot{p}_{XIF}) and ingestion (\dot{p}_{XII}) rates of the mussel, following Saraiva et al. (2011a), with MPs represented by the silt variable. In this approach, a pre-ingestive selection occurs between filtration and ingestion, returning the rejected material in the water through pseudofaeces (J_{pfi}). Consequently, energy is assimilated through food while the non-assimilated particles are excreted through the faeces production (J_f). The model's equations, variables and parameters are shown in Table 1, 2 and 3 respectively. The scaled functional response f (Eq. 5, Table 1), which regulates the assimilation rate, is modified following Kooijman (2006) to include an inorganic term representing the non-digestible matter i.e. microplastics: $f = X/(X + K_y)$ and $K_y = X_K \cdot (1 + Y/Y_K)$ where Y and Y_K are the concentration of MPs, converted from particles L^{-1} to g m^{-3} (Everaert et al., 2018) and





the half saturation coefficient of inorganic particles here represented by MPs (g m^{-3}), respectively. Thus, the assimilation rate that is regulated by f is decreasing when the concentration of MPs is increased. The same approach is followed by other authors who considered inedible particles in the mussel's diet (Ren, 2009, Troost et al., 2010). During the filtration process the same clearance rate for all particles is used ($\{\dot{C}_R\}$), representing the same searching rate for food that depends on the organism maximum capacity ($\{\dot{C}_{Rm}\}$) and environmental particle concentrations (Vahl, 1972, Widdows et al., 1979, Cucci et al., 1989). During the ingestion process the mussel is able to selectively ingest food particles and reject inedible material, in order to increase the organic content of the ingested material (Kjørboe & Møhlenberg, 1981, Jørgensen et al., 1990, Prins et al., 1991, Maire et al., 2007, Ren, 2009, Saraiva et al., 2011a). This selection is reflected by the different binding probabilities adopted for each type of particle (ρ_I for algae particles and ρ_2 for inorganic particles i.e. MPs, see Eq. 14 and table 3). The equations representing the feeding processes handle each type of particle separately, while there is interference between the simultaneous handling of different particle types (Eq. 12-14, Table 1) (Saraiva et al., 2011a). Finally, during the assimilation process, suspended matter (i.e. MPs) that the mussel is not able to assimilate due to its different chemical composition from the reserve compartment (Saraiva et al., 2011a) or incipient saturation at high algal concentrations (Riisgard et al., 2011) results in the faeces production (Eq. 16, Table 1).

2.3 Microplastics accumulation sub-model

With the DEB model as a basis, a sub-model describing the microplastics (MPs) accumulation by the mussel was developed, assuming that the presence of MPs in the ambient water does not cause a significant adverse effect on the organisms' overall energy budget, in accordance with laboratory experiments, conducted in mussel species (Van Cauwenberghe et al., 2015: *Mytilus edulis*, Santana et al., 2018: mussel *Perna perna*). Additionally, it was assumed that the mussel filtrates MPs present in the water, without the ability of selecting between the high energetic valued particles and the MPs during the filtration process (Van Cauwenberghe et al., 2015, Von Moos et al., 2012, Browne et al., 2008, Digka et al., 2018a among others). The uptake of MPs from the environment is taken into account through the process of clearance/filtration rate, while the excretion of the contaminant is derived from two processes: (i) pseudofaeces production and (ii) faeces production. The resulting MPs accumulation is influenced by external environmental factors (MPs concentration, food availability, temperature) and internal biological processes (clearance, filtration, ingestion, growth). All these are described by the following differential equation:



$$\frac{dC}{dt} = C_{env} \cdot \dot{C}_R - \int_{pf2} - \frac{j_f}{p_{x1l}} \cdot C \quad (\text{Eq. 18})$$

where \dot{C}_R is the clearance rate for water (L h^{-1}), containing a concentration of MPs C_{env} (particles L^{-1}). The terms of \int_{pf2} and $\frac{j_f}{p_{x1l}}$ represent the elimination rate of MPs through pseudofaeces and the non-dimensional rate of faeces production with respect to the ingestion rate, respectively (see Table 1, Eq. 15-16). In this context, the pseudofaeces production incorporates the rejected MPs prior to the ingestion, while the faeces production includes MPs that are rejected along with the food particles that are not assimilated by the mussel.

The accumulation of MPs in the individual is represented by the state variable C (particles individual $^{-1}$) which is computed at every model time step. This has been set to one hour, in order to properly resolve the dynamics of the rapidly changing processes, such as feeding and excretion.

2.4 Environmental drivers

Besides MPs concentration in the seawater, the DEB model is forced by sea surface temperature (SST) and food availability, defined as chlorophyll concentration (CHL-a). Hatzonikolakis et al. (2017) have tested the performance of the model, considering also particulate organic carbon (POC) in the mussel's diet, which, however, did not have an important impact on the model's skill against field data. Thus, only CHL-a, is considered as the available food source. For both study areas SST and CHL-a are derived from daily satellite data, a method also used by other authors (i.e. Thomas et al., 2011, Monaco & McQuaid, 2018).

In the North Sea, SST data were obtained from daily satellite images provided by Copernicus Marine Environmental Monitoring Service (CMEMS) at 0.04 degree spatial resolution and CHL-a data from the daily multi-sensor product provided by CMEMS- Globcolour database at 1 km spatial resolution (<http://marine.copernicus.eu/>, generated using CMEMS Products, production center ACRI-ST). The environmental forcing data (SST, CHL-a) were averaged over the study area (51.08° - 51.44° N, 2.19° - 3.45° E), covering the period 2007-2011 (5 years), in order to realistically simulate the wild mussel's growth harvested at late summer 2011 (Van Cauwenberghe et al., 2015).

In the North Ionian Sea, daily satellite SST data were also obtained from the CMEMS database for the Mediterranean Sea with 0.04 degree spatial resolution, while CHL-a data were derived from the merged product of many satellites (i.e. SeaWiFs, Meris, Modis, Viirs and Olci-a) provided by Globcolour web interface (<http://globcolour.info>) at a daily temporal resolution and 1 km spatial resolution. The forcing data were averaged over the study area (39.49° - 39.65° N, 20.09° - 20.23° E) covering the period 2014-2015 (2 years), when the cultured mussel is ready for the market. The satellite derived CHL-a data were estimated based on the OC5 algorithm of Gohin et



al. (2002) in both study areas, which is regarded as suitable for coastal waters. Satellite data have facilitated large scale ecological studies by providing maps of phytoplankton functional types and sea surface temperature (Raitos et al., 2005, 2008, 2012, 2014, Palacz et al., 2013). The daily environmental forcing data are shown in Fig. 1 and Fig. 2 for the North Sea and the N. Ionian Sea, respectively. The two coastal environments present some important differences regarding both CHL-a and SST. Specifically, in the N. Ionian Sea, CHL-a is relatively low (annual mean $\sim 0.88 \text{ mg chl-a m}^{-3}$) and peaks during winter (maximum $\sim 2.64 \text{ mg chl-a m}^{-3}$ at December 2014), while in the North Sea CHL-a is about four times higher (annual mean $4.25 \text{ mg chl-a m}^{-3}$), peaking in April every year (maximum range $29.44\text{--}33.38 \text{ mg chl-a m}^{-3}$), as soon as light availability reaches a critical level (Van Beusekom et al., 2009). The higher productivity in the North Sea is related with the nutrient inputs from the English Channel, the North Atlantic and particularly the river discharge of nutrient-rich waters along the Belgian-French-Dutch coastline, that peaks during winter period (Van Beusekom et al., 2009). The sea surface temperature peaks during August in both areas (Fig. 1 and Fig. 2), but is significantly higher in the N. Ionian Sea (maximum 28.8°C), as compared to the North Sea (maximum $18\text{--}19.3^{\circ}\text{C}$).

The environmental concentration of MPs, C_{env} (particles L^{-1}) was obtained also at a daily time step as randomly generated values of the Gaussian distribution that is determined by the mean value and standard deviation of the observed field data (0.4 ± 0.3 particles L^{-1} , North Sea, Van Cauwenberghe et al., 2015, 0.0012 ± 0.024 particles L^{-1} , N. Ionian Sea, Digka et al., 2018a). Considering that these values originate from surface waters and that mussels live in the near surface layer (0-5 m), C_{env} is estimated as a mean value of the upper layer with the methods described by Kooi et al. (2016), who studied the vertical distribution of MPs, considering an exponential decrease with depth. Specifically, in the N. Ionian Sea, mussels were collected from a depth up to 3 m (Digka et al., 2018a), while in the North Sea (Van Cauwenberghe et al., 2015), there is no information and thus a maximum depth of 5 m is adopted.

In the North Sea simulation, the effect of tides is taken into account by considering that the mussel originated from the intertidal zone, is submerged 12 hours during the day (Van Cauwenberghe et al., 2015). In the N. Ionian Sea simulation, tides are not considered, given the very small tide amplitude (few centimeters) in the Mediterranean (i.e. Sara et al., 2011; Hatzonikolakis et al., 2017) and thus the cultured mussel is assumed permanently submerged. *In situ* hourly tide data (2007-2011) from the coastal zone of the region (Dunkerque station N 51.04820° , E 2.36650°) obtained from Coriolis and Copernicus data provider (<http://marine.copernicus.eu>, <http://www.coriolis.eu.org>), showed that mussels experience alternating periods of aerial exposure and submergence at approximately every 6 hours (2 high and 2 low tides). During aerial exposure the model suspends the feeding processes (Sara et al., 2011)



and simulates metabolic depression (Monaco & McQuaid, 2018) where, the Arrhenius thermal sensitivity equation (Eq. 9) is corrected by a metabolic depression constant ($M_d = 0.15$), a value representative for *M. galloprovincialis* and here applied also for *M. edulis*. In the present study, the mussel's body temperature change during low tide is ignored, inducing a model error. The mussel's body temperature (i.e. surrounding water temperature for submerged mussels) during air exposure depends on many factors, such as solar radiation, air's temperature, wind speed and wave height, according to studies investigating the temperature effect on intertidal mussels (Kearney et al., 2010, Sara et al., 2011). However, the present study aims to primarily examine the MPs accumulation and thus the intertidal mussel's body temperature was not thoroughly examined. Nonetheless, the time that the mussel is able to filter, ingest and excrete the suspended matter (i.e. food and MPs particles) and the effect on the mussel's growth through the modified relation of $k(T)$ are included, since the assimilation process occurs whether the mussel is submerged or not (Kearney et al., 2010).

2.5 Parameter values

Most of the DEB model parameters were obtained from Van der Veer et al. (2006) and are referred to the blue mussel *Mytilus edulis* in the northeast Atlantic (see Table 3 for the exceptions). This assumption has also been adopted in previous studies which showed that this parameter set for *M. edulis* applies also for *M. galloprovincialis* (i.e. Casas and Bacher, 2006, Hatzonikolakis et al., 2017). The half saturation coefficient X_k represents the density of food at which the food uptake rate reaches half of its maximum value and should be treated as a site – specific parameter (Troost et al., 2010, Pouvreau et al., 2006). In order to estimate the value of X_k , a different approach was followed for each study area.

For the North Sea simulation, X_k was tuned so that the simulated individual has the recorded size at the corresponding estimated age (Van Cauwenberghe et al., 2015) growing with the representative growth rates of wild *M. edulis* at the region (Saraiva et al., 2012, Sukhotin et al., 2007). For the N. Ionian Sea simulation, an alternative method was adopted, aiming to generalize the DEB model to overcome the problem of site-specific parameterization. The DEB model was tuned against literature field data for cultured mussels originated from different areas in the Mediterranean and Black Seas, where the average CHL-a concentration ranged between 1.0 and 5.0 mg chl-a m⁻³, and one X_k value was found for each area. The four areas used, their characteristics and the corresponding value of X_k adopted, are shown in Table 4. These values of X_k are related to the prevailing CHL-a concentration of each area ([CHL-a]) through three different functions: linear: $f(x) = a * [CHL - a] + b$ exponential: $f(x) = a * \exp(b * [CHL - a])$ and power: $f(x) = a * [CHL - a]^b + c$. The curve fitting app of Matlab (Matlab R2015a) was used for the



determination of a , b and c of each function taking into account the 95% confidence level. The score of each function regarding the somatic/mussel growth simulation in all four regions is tested through target diagrams (Jolliff et al., 2009) by computing the bias and unbiased root-mean-square-deviation (RMSD) between field and simulated data of all 4 regions and the function with the best score is adopted. A similar approach was followed by Alunno-Bruscia et al. (2011) for the oyster *Crassostrea gigas* in six Atlantic ecosystems who expressed the X_k as a linear function of food density (e.g. phytoplankton). Unfortunately, the approach described for the N. Ionian Sea simulation could not be applied in the North Sea, as the limited amount of growth data from the literature for wild *M. edulis* in similar environments did not permit a statistically significant fit of a similar function ($X_k = f(chl - a)$).

2.6 Simulation of reproduction-Initialization of the model

The reproductive buffer (R) is assumed to be completely emptied at spawning ($R = 0$) (Sprung, 1983, Van Haren et al., 1994). In order to simulate mussel's spawning, the gonado-somatic index (GSI) defined as gonad dry mass over total dry flesh mass was computed at every model's time step (Eq. 17 Table 1; the water content of the fresh tissue mass was assumed 80% according to Thomas et al. (2011)). Spawning was induced by a critical value of GSI (GSI_{th} , Table 3) and a minimum temperature threshold (T_{th}) at each study area, obtained from the literature. In the North Sea implementation, T_{th} was set at 9.6 °C (Saraiva et al., 2012), while in the N. Ionian Sea, at 15 °C (Honkoop and Van der Meer, 1998). This kind of formulation for the spawning event in bivalves has been used in previous studies (i.e. Pouvreau et al., 2006, Troost et al., 2010, Thomas et al., 2011, Monaco & McQuaid, 2018). The simulated abrupt losses of the mussel's tissue mass correspond to spawning events and the model's prediction was compared with the available literature data regarding the spawning period in each study area. Theodorou et al. (2011) demonstrated that the spawning events occur during winter for *M. galloprovincialis* in the mussel farms of Greece, while in the North Sea the spawning period for *M. edulis* is extended from the end of April until the end of June (Sprung, 1983, Cardoso et al., 2007).

In both areas, the model was initialized so that the simulated individual is in the juvenile phase ($V < V_p$; Table 3) and the reproductive buffer can be considered to be empty ($R = 0$) (Thomas et al., 2011). As stated by Jacobs et al. (2015) amongst others, juvenile mussels (*M. edulis*) range between 1.5-25 mm in size. Specifically, in the North Sea the settlement of mussel larvae (*M. edulis*) takes place in June and the juveniles grow to a maximum size of 25 mm within 4 months (Jacobs et al., 2014). In the N. Ionian Sea, the operating mussel farms follow the life cycle of *M.*



galloprovincialis, starting the operational cycle each year by dropping seed collectors from late November until March and the juvenile mussels grow up to 6-6.5cm after approximately one year according to the information obtained from the local farms in the region and Theodorou et al. (2011). The initial fresh tissue mass was distributed between the structural volume (V) and reserves energy (E). Energy allocated to those two compartments was firstly constrained by the initial length (L) and then energy allocated to V was in Eq.10 (Table 1). The initial value of E was set so that the simulated individual has an initial weight that corresponds to the juvenile phase ($V < V_p$) (Table 5). Finally, for both model implementations, the initial accumulation of MPs in the mussel's tissue (C) was set to zero.

2.7 Simulation Runs

The DEB-accumulation model simulates at an hourly basis the growth and MPs accumulation of the wild mussel from the North Sea and the cultured mussel from the N. Ionian Sea. Initially, a model run is performed at each study area during the periods July 2007 to August 2011 (4 years) for the North Sea simulation and late November 2014 to January 2016 (~ 1 year) for the N. Ionian Sea simulation. Additionally, the inverse simulations were performed in order to evaluate the depuration phase of both cultured and wild mussel, by setting the environmental MPs concentration equal to zero ($C_{env}=0$), after a period of 1 year simulation at the N. Ionian Sea, when the cultured mussel has the appropriate size for market, and after 4 years at the North Sea, when literature field data are available (Van Cauwenberghe et al., 2015). In this simulation, the mussel's gut clearance is achieved by the excretion of MPs through faeces (3rd term of Eq. 18), and thus it is necessary to maintain the existence of food in the mussel's environment in order to ensure that the feeding-excretion processes will occur.

Furthermore, to examine the model's uncertainty related to the environmental MPs concentration, a series of 15 and 13 simulations were performed in the North Sea and N. Ionian Sea respectively, adopting different constant values of C_{env} within the observed range of each area. Finally, the effect of the environmental forcing data and some model's parameters on the resulting MPs accumulation by both mussels is explored through sensitivity experiments. These were used to derive a new function that predicts the level of MPs pollution in the environment.

2.8 Sensitivity tests and Regression analysis



The effect of the environmental data (CHL-a, temperature, C_{env}) and two parameters representative of mussel's growth (X_k , Y_k) on the MPs accumulation by the mussel for each study area was examined through sensitivity experiments with the DEB-accumulation model. Each variable (CHL-a, T , C_{env}) and parameter (X_k , Y_k) was perturbed by $\pm 10\%$ and the results of each run were analyzed using the sensitivity index (SI), which calculates the percentage change of the mussel's MPs accumulation $SI = \frac{1}{n} \sum_{t=1}^n \frac{|C_t^1 - C_t^0|}{C_t^0} \cdot 100$ (%), where n is the simulated time steps, C_t^0 is the MPs accumulation predicted with the standard simulation at time t and C_t^1 is the MPs accumulation with a perturbed variable/parameter at time t ; for details see Bacher and Gangnery, (2006). In order to also examine the effect of tides, in the North Sea implementation, the sensitivity experiments were conducted twice: the first time assuming that the mussel is permanently submerged and the second time assuming that the mussel is periodically exposed to the air.

Preliminary sensitivity experiments showed that the MPs accumulation is highly depended on the prevailing conditions regarding the CHL-a, temperature and C_{env} and the mussel's growth that is regulated by the half saturation coefficient (X_k). Therefore an attempt was made using the model's output to describe the MPs accumulation as a function of these variables through a custom regression model:

$$y = b_1 * W + b_2 * \exp\left(\frac{1}{T}\right) + b_3 * \frac{1}{[CHL-a]} + b_4 * C_{env} \quad (\text{Eq. 19})$$

where y (particles/individual) is the response variable and represent the predicted MPs accumulation by the mussel; W (g) the mussel's fresh tissue mass, T (K) the sea surface temperature, CHL-a and C_{env} are the concentrations of chlorophyll-a and MPs in the water respectively, which are the predictor variables. The values of coefficients b_1 , b_2 , b_3 , and b_4 are calculated using the nonlinear regression function (nlinfit, Matlab R2015a) which attempts to find values of the parameters b that minimize the least squared differences between the model's MPs accumulation output C and the predictions of the regression model $y = f(W, T, [chl\ a], C_{env}, b)$.

The ultimate aim of this analysis, once coefficients are determined, is to use equation 19 to obtain the environmental MPs concentration:

$$C_{env} = \frac{1}{b_4} * \left(C - b_1 * W - b_2 * \exp\left(\frac{1}{T}\right) - b_3 * \frac{1}{[CHL-a]} \right) \quad (\text{Eq. 20})$$

which could be a very useful tool to predict the MPs concentration in the environment, when all involved variables are known (mussel size, accumulated MPs, temperature and CHL-a), using the



mussel as a potential bioindicator (Li et al., 2016, Li et al., 2019). The score of this custom model was tested by applying Eq. 20 in our study areas and 6 more areas around the U.K., where information of mussel's wet weight and both mussels' and environment's MPs load is available (Li et al., 2018). CHL-a and temperature, which were not included in Li et al. (2018), were obtained from daily satellite images (same source as in the North Sea, see 2.4 section), covering the period that the mussels were harvested (Li et al., 2018).

3. Results

3.1 Growth simulations

The growth simulations of *M. edulis* and *M. galloprovincialis* for the North Sea and the N. Ionian Sea are shown in Fig. 4 and Fig. 5 respectively. In the North Sea implementation, X_k was tuned to a constant value: $X_k=8 \text{ mg chl-a m}^{-3}$. The fitted value was slightly higher, as compared to the one ($X_k=3.88 \text{ } \mu\text{g chl-a l}^{-1}$) used by Casas and Bacher (2006) in productive areas of the French Mediterranean shoreline (average CHL-a concentration $1.45 \text{ } \mu\text{g chl-a l}^{-1}$ maximum peak at $20 \text{ } \mu\text{g chl-a l}^{-1}$), given the even higher productivity in the North Sea (average CHL-a concentration $4.25 \text{ } \mu\text{g chl-a l}^{-1}$; maximum peak at $\sim 33.40 \text{ } \mu\text{g chl-a l}^{-1}$). The high value of X_k could also be explained by the presence of silt and other inedible particles (i.e. MPs) which result to lower quality food in the mussel's diet compared with a "clean" site (Kooijman, 2006, Ren, 2009). Furthermore, it has been reported that wild mussels grow considerably slower than farmed mussels (~ 1.7 times) (Sukhotin and Kulakowski, 1992) and thus, a higher value of X_k promotes a lower mussel growth, which is the case of the North Sea mussel. The simulated mussel shell length after 4 years, in August, is 4.35 cm and the fresh tissue mass is 1.87 gr, in agreement with Van Cauwenberghe et al. (2015) and other studies conducted on wild mussels (Sukhotin et al., 2007, Saraiva et al., 2012, MarLIN, 2016). In particular, Saraiva et al. (2012) found that after 16 years of simulation, the wild mussel of the Wadden Sea (North Sea) is 7 cm long, while according to Bayne and Worrall (1980) a mussel with shell length 4 cm corresponds to the age of 4 years, in agreement with the current study. The simulated growth presents a strong seasonal pattern, being higher during spring and summer season, as compared to autumn and winter, which is consistent with the seasonal cycle of temperature and CHL-a concentration, for a typical year in the region (Fig. 1). The increase of food availability and temperature during spring (April) results in high mussel growth for a 4-month period, while the decrease of CHL-a from summer until the end of the year, in conjunction with the temperature



decrease in autumn, result in a lower mussel growth. Spawning events occurred between the end of April and beginning of May (30 April–2 May) each year, are responsible for the sharp decline in mussel's fresh tissue mass, shown in Fig. 4 (Handa et al., 2011; Zaldivar, 2008) and in agreement with the literature (Sprung, 1983, Cardoso et al., 2007, Saraiva et al., 2012). The predicted weight loss due to spawning was around 7% at the first year of simulation, while the second, third and fourth year the percentage of weight loss increased gradually to 8.3%, 12.6% and 14.4% respectively. Bayne and Worrall (1980) demonstrated that the weight losses on spawning for individuals of 1 g weight vary between 2.1% and 39.8%, presenting a weight-specific increase with size.

In the N. Ionian Sea implementation, X_k is applied as a function of CHL-a concentration through the method described in section 2.5. The target diagram showing the performance of each tested function (linear: $f(x) = a * [CHL - a] + b$, where $a = 0.959$ and $b = -1.420$; exponential: $f(x) = a * \exp(b * [CHL - a])$ where $a = 0.2$ and $b = 0.567$; power: $f(x) = a * [CHL - a]^b + c$ where $a = 0.01$, $b = 3.529$ and $c = 0.480$) is shown in figure 3. The linear and power function of X_k present a good skill, with the power function leading to the most successful simulation of the cultured mussel's growth in all four areas (diagram marks for mussel length and fresh tissue mass are closer to the target's center). The power function applied in the N. Ionian Sea, resulted in mussel's shell length 5.8 cm and fresh tissue mass 5.92 gr after one year simulation, in agreement with Theodorou et al. (2011). The spawning event occurred at the beginning of December (Theodorou et al., 2011) and was illustrated by 12.6% tissue mass decline.

3.2 Microplastics accumulation and depuration phase

The hourly simulated MPs accumulation by the mussel in the North Sea and N. Ionian Sea are shown in Fig. 6 and Fig. 7 respectively. In the North Sea, a 4-year-old wild mussel ($L=4.35$ cm, $W=1.87$ g) contains 0.64 particles individual⁻¹ in August within the range value found by Van Cauwenberghe et al. (2015) (0.4 ± 0.3 particles individual⁻¹). It is worth noting that Van Cauwenberghe et al. (2015) allowed a 24 h clearance period, before analyzing mussels' tissue for MPs, possibly resulting in slightly lower MPs accumulation than the model's prediction. In the N. Ionian Sea, the simulated MPs accumulation by the cultured mussel with $L=4.88$ cm and $W=3.43$ g was 0.91 particles individual⁻¹ in July, in agreement with field observations obtained from Digka et al. (2018a) (0.9 ± 0.2 particles individual⁻¹). In both regions, the model computed MPs accumulation, assuming that the mussel treats MPs as silt particles (i.e. inedible particles) and is in agreement with the available field data. This suggests that mussels probably present a common





behavior against all inedible particles. In model's results, based on the uptake and excretion rates of MPs by the mussels in both study areas, the majority of MPs are rejected through pseudofaeces and fewer through faeces production (not shown). This is in agreement with Woods et al. (2018) who found that most microplastic fibers (71%) were quickly rejected as pseudofaeces and < 1% excreted in faeces.

The small-scale fluctuations of MPs in the mussel (wild and cultivated) reflect the adopted random variability of the environmental MPs concentration C_{env} and the daily environmental forcing (CHL-a, temperature). The large-scale (seasonal) variability follows mainly the variability of the clearance rate. The seasonal variability of the CHL-a concentration and temperature greatly determines the variability of the clearance rate and hence the variability of MPs in the individual. Moreover, the model predicts that mussel's energy needs are increased as it grows and therefore the clearance rate is increased, resulting in higher MPs accumulation.

The simulated time needed to clean the mussel's gut from the MPs load for both areas is shown in Fig. 8. In both areas, the cleaning follows an exponential decay, in agreement with Woods et al. (2018). In particular, the model predicts a 90% mussel's cleaning after 330 hours (~14 days) and 63 hours (~3 days) for the N. Ionian Sea and North Sea respectively. The cleaning process is more rapid in the North Sea simulation, which can be attributed to the higher CHL-a concentration found in this area, leading to increased production of faeces by the mussel and hence faster excretion of the accumulated MPs. In the N. Ionian Sea, on the other hand, the rate of the mussel's cleaning is slower, due to the limited food availability.

3.3 Model's uncertainty regarding the environmental microplastics concentration

The MPs concentration in the environment presents a strong variability in both temporal and spatial scales. To examine the model's uncertainty related to the environmental MPs concentration (C_{env}), a series of 15 and 13 simulations were performed in the North Sea and N. Ionian Sea respectively, adopting different values of C_{env} within the observed range of each area. In the North Sea, the adopted C_{env} ranged between 0.1 and 0.8 particles L^{-1} with a step of 0.05 (15 runs), while in the N. Ionian Sea C_{env} ranged between 0.0012 and 0.0252 particles L^{-1} with a step of 0.002 (13 runs). The mean seasonal values and standard deviation of the 15 simulations in the North Sea and the mean monthly values and standard deviation of the 13 simulations in the N. Ionian Sea were computed and plotted in Fig. 9 and Fig. 10, respectively. Each error bar represents the uncertainty of the simulated accumulation at the specific time, related to the environmental MPs concentration.



In both case studies, the uncertainty of the model appears to increase as the MPs accumulation is increased. As the mussel grows in the North Sea, the mean value and standard deviation of MPs accumulation is increased during the same season every year, illustrating the effect of the mussel's weight. Moreover, the seasonal variability of the MPs accumulation should be caused by the seasonality of CHL-a concentration. This is apparent during each year's spring: when CHL-a concentration peaks at its maximum value ($\sim 30 \text{ mg m}^{-3}$; see Fig. 1), the filtration rate is decreased (Riisgard et al., 2003, 2011), leading to lower MPs accumulation by the mussel and thus lower model's uncertainty. In the N. Ionian Sea, the effect of the mussel's weight is more apparent in the early months (~ 6 months), resulting on higher MPs accumulation and model uncertainty as the mussel grows. Afterwards, the seasonality of both CHL-a concentration and temperature plays the major role. During summer, when the CHL-a concentration is progressively decreased, reaching minimum values ($\sim 0.7 \text{ mg /m}^3$) and temperature is increased ($>20^\circ \text{ C}$), the filtration rate is significantly decreased or stopped, resulting in lower MPs accumulation and lower model's uncertainty. This is in line with studies reporting that the mussel suspends the filtering activity and thus closes its valves until better conditions occur (Pascoe et al., 2009, Riisgard et al., 2011). Overall, the available field data lie within the model's uncertainty for both study areas.

Moreover, to evaluate the scenario adopted with the set-up of the previous experiments (random C_{env} at a daily time step) 3 additional model runs are performed in each study area, adopting each time different stochastic sequences of daily random C_{env} values within the observed range, which is considered to reflect the high spatial and temporal variability of the environmental MPs concentration. The mean value and standard deviation of these "stochastic" runs lie most of the time within the standard deviation of the overall model's uncertainty in both case study areas (Fig. 9 and Fig. 10).



3.4 Sensitivity and Regression analysis results

The results of the sensitivity experiments regarding the MPs accumulation by the mussels are shown in Fig. 11 and 12 for the North Sea and N. Ionian Sea respectively. The comparison between the intertidal and subtidal mussel of the North Sea revealed that both +10% and -10% perturbation of CHL-a and X_k have a slightly lower effect on the MPs accumulation by the intertidal mussel which is probably attributed to the intermittent feeding periods experienced by the individual due to the tide effect. As far as the temperature effect, both +10% and -10% perturbed value led to higher sensitivity on the MPs accumulation by the intertidal mussel, due to the adopted modified temperature relation during low tide. Especially, if the mussel's body temperature change during air



exposure would be considered, the perturbed temperature will probably affect even more the MPs accumulation on the intertidal than the subtidal mussel. The effect of the C_{env} is slightly higher and lower on the MPs accumulation by the intertidal mussel when perturbed +10% and -10% respectively, however the difference of the sensitivity index (%) between the two mussels (intertidal vs. subtidal) is small, indicating that the environmental MPs concentration affects similarly both mussels, regardless the continuous or intermittent feeding-excretion process.

The comparison between the mussel sensitivity indexes in the N. Ionian and the North Sea (in conditions of submergence) study areas reveals some important differences. Generally, most of the perturbed (either +10% or -10%) variables and parameters (i.e. CHL-a, temperature, X_k) present higher sensitivity on the MPs accumulation by the mussel from the N. Ionian Sea. This is attributed to the prevailing environmental conditions and specifically the lower food availability (CHL-a) and the higher temperature range in the N. Ionian Sea compared to the North Sea, which greatly determine the feeding processes, the mussel's growth and hence the MPs accumulation. The perturbed C_{env} in both study areas appears to affect similarly the MPs accumulation on both mussels (-10%), with the small difference probably attributed to the higher abundance of seawater's MPs present in the North Sea compared to the N. Ionian Sea. Finally, the half saturation coefficient for the inorganic particles (Y_k) has no effect on the MPs accumulation of both North Sea and N. Ionian Sea mussels, indicating that the amount of inedible particles (i.e. MPs) is relatively low in both areas and thus the Y_k does not affect the way that the organic particles are being ingested (Kooijman, 2006). According to Ren (2009), when the inorganic matter is low, the $K(y)$ (Eq. 5; Table 1) is approximately equal to X_k and then Y_k is the least sensitive parameter for the ingestion rate and thus growth.

The DEB-accumulation model output was used to determine the coefficients in Eq. 19 by the nonlinear regression analysis: $b_1 = 0.1909 (\pm 0.0006)$, $b_2 = 0.0412 (\pm 0.0019)$, $b_3 = 0.1315 (\pm 0.00)$ and $b_4 = 1.1060 (\pm 0.0253)$. The confidence intervals for the estimated coefficients (b_1 , b_2 , b_3 , b_4) are small enough which indicates an accurate estimation of them and the mean squared error of the regression model is small enough (MSE=0.0523). Subsequently, as shown in Figure 13, Equation 20 may be used to predict the MPs concentration of the environment where mussels live, being in most cases within the standard deviation of the field data. However, this is just a rough demonstration of the method and should be implemented in more environments in order to be further validated.





4. Discussion

A DEB-accumulation model was developed and validated with the ~~only available~~ data from the North Sea and the N. Ionian Sea, to study the MPs accumulation by wild *M. edulis* and cultured *M. galloprovincialis*, ~~as they~~ grow in different environments. Although the study is limited by scarce validation data, it is notable that the accumulation submodel's parameters are extracted from literature (Table 3) illustrating that mussels adopt a common defensive mechanism against inedible particles (i.e. silt, MPs). Thus, the theoretical background constructed by Saraiva et al., (2011a) (based on Kooijman, 2010) regarding the feeding and excretion processes of the mussel remains unspoiled. Through the strong theoretical background of DEB theory, this study highlights that the accumulation of MPs by the mussel is highly depended on the prevailing environmental conditions which control the amount of MPs that the mussel filtrates and excretes.

Beginning with the generalization of the DEB model regarding the site-specific parameter X_k in the N. Ionian Sea simulation, the function of the half saturation ($f(x) = a * [CHL - a]^b + c$) successfully captures the physiological responses and thus the growth rate of the cultured mussel. In the current study, ~~a demonstration of this method is conducted leading to a DEB growth model robust enough with a sufficiently generic nature for the simulation of~~ the mussel growth in representative mussel habitats of the Mediterranean Sea, covering a range of productivity and sea surface temperature. Bourles et al. (2008) suggested for oyster growth (*Crassostrea gigas*) that a seasonally varied half saturation coefficient could improve the accuracy of the food quantifier because seawater composition is closely related to the season. As more field data becomes available from various environments, such an approach could result to more generic formulations for the site-specific parameter X_k , so that the model could be applied in several areas of interest, where field growth data are absent and/or to simulate the potential mussel growth in the 2D space.

The simulation of MPs accumulation by the mussels, using the DEB-accumulation model, is in good agreement with the available field data. The MPs accumulation by the cultivated mussel (fresh tissue mass 3.42 g) originated from the N. Ionian Sea with mean $C_{env} = 0.0012 \pm 0.024$ particles L^{-1} , is 0.91 particles individual⁻¹ and by the wild mussel (fresh tissue mass 1.87 g) from the North Sea with mean $C_{env} = 0.4 \pm 0.3$ particles L^{-1} is 0.64 particles individual⁻¹. If these concentrations are expressed per gram of wet tissue of mussels, the cultivated mussel contamination (0.27 particles $g^{-1}w.w.$) is comparable with the wild mussel (0.34 particles $g^{-1}w.w.$), despite the much lower environmental MPs concentration (C_{env}) in the N. Ionian Sea than the North Sea. This comparison aims to highlight the significant impact of the prevailing environmental conditions (CHL-a and temperature) on the MPs accumulation by the mussels, although they originate from





different areas and lived different time period. The generally high abundance of CHL-a in the North Sea simulation, contributes to a reduction of the filtering activity and hence of the MPs accumulation. The threshold algal concentration for reduction of the mussel's filtration rate (incipient saturation) has been found to lie between 6.3 and 10.0 $\mu\text{g chl a L}^{-1}$ (Riisgard et al., 2011), which is the North Sea case. Furthermore, in the N. Ionian Sea simulation, the filtration, ingestion, pseudofaeces and faeces production rates are decreased during the summer season when the CHL-a and temperature has downward and upward trend respectively, gradually leading to a decline of the mussel's MPs accumulation. Van Cauwenberghe and Janssen (2014) found that cultivated *M. edulis* from the North Sea contained on average 0.36 ± 0.07 particles $\text{g}^{-1}\text{w.w.}$, a similar value with that found in the present study for the wild mussel of the North Sea (0.34 particles $\text{g}^{-1}\text{w.w.}$). This probably highlights the small contribution of mussel farms as a source of MPs pollution (Santana et al., 2018). Moreover, the intertidal wild mussel (present study) is assumed to filter and excrete MPs half of the time in comparison with the submerged cultured mussel in the North Sea, resulting though in similar accumulation level. The model also predicts the time needed for the 90% gut clearance of both cultured (N. Ionian Sea) and wild (North Sea) mussel to be almost 330 hours and 63 hours (equivalent to 14 and 3 days) respectively, when MPs contamination is removed from their habitat. This is in line with a series of studies which demonstrated that the depuration time varies between 6-72 hours and can last up to 40 days depending on several factors such as species, environmental conditions (Bayne et al., 1987), size and type of MPs (Browne et al., 2008, Ward and Kach, 2009, Woods et al., 2018, Birnstiel et al., 2019).

The strong dependence of food (CHL-a), temperature and seawater's MPs concentration on the MPs accumulation by the mussel, regarding its wet weight, is demonstrated through sensitivity experiments that were used to derive a rather simple nonlinear regression model (Eq. 19). The comparison of the regression model's with the DEB model's output resulted in a quite accurate estimation of the coefficients, which in turn sparked the idea of a 'new' relationship (Eq. 20) that could potentially predict the MPs concentration in the environment when certain conditions are known (CHL-a, T, C_{env} , W). The latter equation was applied in 8 areas in total (2 from the present study areas and 6 from Li et al. (2018), with relatively good results since the predicted value is within the observed range of field data in most regions, making the mussel a potential bioindicator. Mussels have been previously proposed as bioindicators for marine microplastic pollution (<1 mm), although the efficient gut clearance and selective feeding behavior limit their quantitative ability (Lusher et al., 2017, Brate et al., 2018, Beyer et al., 2017, Fossi et al., 2018, Li et al., 2019). The very recent study by Ward et al. (2019) demonstrated that bivalves are poor bioindicators of MPs pollution due to the particle selection during feeding and excretion processes that is based on the physical characteristics of the MPs. Considering that the MPs accumulation is site-dependent, and





671 that sampling of mussels is usually easier than seawater (Karlsson et al., 2017, Brate et al., 2018),
672 models like the one described in Eq. 20 that besides the MPs accumulation take into account
673 characteristics of the environment, which are crucial for the way that mussels accumulate MPs,
674 possibly could be used at global level and allow comparisons between various environments.



675 However, the method described should be validated in more environments with more frequent field
676 data to be able to provide secure results.

677 Despite the scarce validation data, in this study there are some other limitations. First of all,
678 the data regarding the concentration of MPs in the mussels' environment is also scarce; since MPs
679 is a relatively recent subject of study, the existing knowledge of the spatial and temporal
680 distribution is still quite limited (Law and Thompson, 2014, Browne, 2015, Anderson et al., 2016,
681 de Sa et al., 2018, Smith et al., 2018, Troost et al., 2018). To overcome the lack of environmental
682 MPs time series, a function of randomly generated values within the observed range of each area
683 was applied and its uncertainty was examined through an ensemble forecasting. Specifically, the
684 model's uncertainty due to the environmental MPs concentration (C_{env}) was tested by performing a
685 series of model runs forced by an envelope of representative values of C_{env} and the results (section
686 3.3) show that the adopted stochastic scenario simulates realistically the MPs accumulation by the
687 mussels and in agreement with the available field data. The approach used is assumed to be close to



688 reality since it has been reported that ~~MPs quantification in the water is rather a complicated~~
689 ~~procedure due to the influence of many factors such as tides, wind, wave action, ocean currents,~~
690 ~~river inputs and hydrodynamic features resulting~~ to high spatially and temporally variability of MPs
691 distribution even in very small scales (Messinetti et al., 2018, Goldstein et al., 2013). In a future
692 work the DEB-accumulation model could be coupled with a high-resolution MPs distribution model
693 (Kalaroni et al., 2019) to overcome this limitation. Moreover, the approach followed in calculating
694 the value of MPs concentration in the near surface layer (0-5m depth) (Kooi et al., 2016), resulted in
695 a representative value of the upper ocean layer. In depth knowledge of the MPs distribution, both
696 horizontally and vertically, is essential to understand and mitigate their impact not only on the
697 various marine compartments but also on the organisms inhabiting those (Van Sebille et al., 2015,
698 Kooi et al., 2016). For that reason, it is important to enhance the monitoring activity especially in
699 the vulnerable coastal environments, adopting integrated cross-disciplinary approaches and
700 monitoring of biological, physical and chemical parameters which provide information on the
701 ecosystem function, in order to improve the assessment of emerging pollutants (i.e. MPs) and their
702 impacts on biota (objective of JERICO-RI framework).



703 Further, the assumption that the mussel has the same filtration rate for all particles
704 independently of their chemical composition, size and shape, is a simplification and a contradictory
705 theme of discussion (see Saraiva et al., 2011a for details). However, through the model, a pre-



ingestive particle selection by the mussel is implied based on the organic-inorganic content of the suspended matter illustrating the different binding probabilities applied for algal and MPs particles during the ingestion process. Through an investigation of wild mussel's faeces and pseudofaeces production in laboratory conditions, Zhao et al. (2018) found that the length of MPs was significantly longer in pseudofaeces than in the digestive gland and faeces. Furthermore, Van Cauwenberghe et al. (2015) demonstrated that mussel's faeces contained larger MPs (15–500 μm) compared to the mussel's tissue (20–90 μm). Apparently, smaller sized MPs seem to be dominant within the mussels in comparison with the ambient environment (Li et al., 2018, Qu et al., 2018, Digka et al., 2018b), implying that the mussel is more prone to ingest and retain smaller sized MPs. As an example, Digka et al. (2018b) confirmed that the smaller MPs (<1 mm) occupy the 62.3%, 96.9% and 100% in seawater, sediments and mussels from the N. Ionian Sea respectively. In a future work this selection pattern regarding size, could be simulated by suitable preference weights among different MPs sizes. This will improve the knowledge of the feeding and excretion mechanisms used by the mussels against MPs pollution and the assessment of the ecological footprint (Rist et al., 2019).

Moreover, the assumption that the contamination by MPs does not affect the energy budget in terms of growth might also be a simplification as this is a subject currently under investigation. Van Cauwenberghe et al. (2015) found that although mussels *M. edulis* exposed to MPs increased their energy consumption, the energy reserves was not affected compared to the control organisms, implying that mussels are able to adopt a defensive mechanism against the suspended inorganic particles (i.e. MPs) (Ward and Shumway, 2004). Furthermore, MPs exposure showed no significant effect on mussel's *Perna perna* energy budget, despite its long duration and relatively realistic intensity, concluding to the assumption of mussel's acclimation to maintain its health (Santana et al., 2018). On the contrary, other authors who mainly intended to predict future effects, suggested a significant energy shift from reproduction to structural growth and elevated maintenance costs, probably attributed to the reduced energy intake, when the organisms (i.e. oyster *Crassostrea gigas*) were contaminated with high and unrealistic concentration of MPs (Sussarellu et al., 2016). Moreover, Gardon et al. (2018) showed that the overall energy balance of oyster *Pinctada margaritifera* was significantly impacted by the reduced assimilation efficiency in correlation with the exposed dose of MPs and for that reason energy had to be withdrawn from reproduction to compensate for the energy loss. In future dedicated experiments exploring the effects on all components of a DEB model should be carried out considering long-term realistic MPs exposure.

Furthermore, the tide data as considered in the present study impose model's bias, since the mussel's body temperature change when exposed to air was not taken into consideration. Assessing mussel's body temperature demand extended experiments in field conditions (Tagliarolo and





741 McQuaid, 2015, Monaco and McQuaid, 2018). A very recent study by Seuront et al. (2019) along
 742 the French coast of the eastern English Channel found no significant correlation between air's and
 743 mussel's body temperature, but rather positively significant correlation with the hard substrate's (i.e.
 744 rocks) temperature. However, in the present study the tide effect on processes that are affected by
 745 the thermal equation ($k(T)$) is considered through the metabolic depression (details in section 2.4).
 746 Sara et al. (2011) following the method developed by Kearney et al. (2010), who coupled a DEB
 747 model with a biophysical model, incorporated the change of mussel's body temperature during
 748 emersion, using information of various climatological variables (i.e. solar radiation, air temperature,
 749 wind speed, wave height), but the temperature sensitivity on the physiological processes was
 750 ignored. In a future study, a similar approach by coupling the present DEB-accumulation model
 751 with a biophysical model could be followed and lead to a more detailed simulation of the mussel's
 752 body temperature.

753 5. Conclusions

754
 755 In a future study the model should be validated against more frequent field data regarding
 756 the MPs accumulation, with sampling of mussels among various sizes and life stages as for now it
 757 cannot be reliable in conducting predictions within accepted precision. However, this study
 758 provides a new approach in studying the accumulation of MPs by filter feeders and reveals the
 759 relations between characteristics of the mussel's surrounding environment and the MPs
 760 accumulation, which is presented with high seasonal fluctuations. Additionally, in a future study the
 761 DEB-accumulation model will be coupled with a coupled hydrodynamic-biochemical model
 762 (Petihakis et al., 2002, 2012, Triantafyllou et al., 2003, Tsiaras et al., 2014, Ciavatta et al., 2019,
 763 Kalaroni et al., 2020) and a MPs distribution model (Kalaroni et al., 2019) that will provide fields of
 764 temperature, food availability and MPs concentration respectively at the Mediterranean scale, and
 765 eventually lead to an integrated representation of the MPs accumulation by mussels (Daewel et al.,
 766 2008). This fully coupled model will be downscaled to the Cretan Sea SuperSite, while the
 767 parameterization of important biological processes will be redesigned based on the new data which
 768 will be acquired in the framework of the JERICO S3 project (<http://www.jerico-ri.eu>). The present
 769 study highlights the urgent need for adopting a multi-disciplinary monitoring activity by measuring
 770 physical, biological and chemical parameters that are crucial for mapping the MPs distribution,
 771 assessing the contamination level of the marine organisms and investigating the impact on the
 772 health status. Overall, despite the significant limitations that were mentioned before, taken into
 773 account that plastics are one of the global hot issues, this particular study could help for the design
 774 of next efforts, since it provides indications on the future priority related issues.



775

776 **Author Contribution:**

777 **Natalia Stamataki, Yannis Hatzonikolakis, Kostas Tsiaras, Catherine Tsangaris, George**
778 **Petihakis, Sarantis Sofianos, George Triantafyllou**

779

780 G.T. conceived the basic idea of the present study and was responsible for the management and
781 coordination of the research planning and execution. N.S. and Y.H. developed the model code with
782 the contribution of K.T.. N.S. collected the existing information on the subject and performed the
783 simulations of the present study with the help of Y.H. when needed. G.T., G.P., K.T., Y.H. and N.S.
784 contributed to the interpretation of the results. C.T. provided the field data of the mussel's
785 microplastic accumulation in the North Ionian Sea. N.S. prepared the manuscript, with critical
786 review, commentary and revision contributed from all co-authors.

787

788 **Competing interests:**

789 The authors declare that they have no conflict of interest.

790

791 **Acknowledgments:**

792

793 This work was partially funded by the national project 'Blue growth with innovation and
794 application in Greek Seas' (MIS 5002438) and the EU H2020 CLAIM project (G.A. n° 774586).
795 This study has been conducted using E.U. Copernicus Marine Service Information
796 (<http://marine.copernicus.eu/>). Part of this work was supported by the JERICO- NEXT project. This
797 project has received funding from the European Union's Horizon 2020
798 research and innovation programme under grant agreement no. 654410.

799

800

801

802

803



References

- Alunno-Bruscia, M., Bourlès, Y., Maurer, D., Robert, S., Mazurié, J., Gangnery, A., Goulletquer, P. and Pouvreau, S.: A single bio-energetics growth and reproduction model for the oyster *Crassostrea gigas* in six Atlantic ecosystems, *J. Sea Res.*, 66(4), 340–348, doi:10.1016/j.seares.2011.07.008, 2011.
- Anderson, J. C., Park, B. J. and Palace, V. P.: Microplastics in aquatic environments: Implications for Canadian ecosystems, *Environ. Pollut.*, 218, 269–280, doi:10.1016/j.envpol.2016.06.074, 2016.
- Andrady, A. L.: Microplastics in the marine environment, *Mar. Pollut. Bull.*, 62(8), 1596–1605, doi:10.1016/j.marpolbul.2011.05.030, 2011.
- Arthur, C., J. Baker and H. Bamford (eds). Proceedings of the International Research Workshop on the Occurrence, Effects and Fate of Microplastic Marine Debris. Sept 9–11, 2008. NOAA Technical Memorandum NOS-OR&R-30, 2009
- Bacher, C. and Gangnery, A.: Use of dynamic energy budget and individual based models to simulate the dynamics of cultivated oyster populations, *J. Sea Res.*, 56(2), 140–155, doi:10.1016/j.seares.2006.03.004, 2006.
- Bayne, B. and Worrall, C.: Growth and Production of Mussels *Mytilus edulis* from Two Populations, *Mar. Ecol. Prog. Ser.*, 3, 317–328, doi:10.3354/meps003317, 1980.
- Bayne, B. L., Hawkins, A. J. S. and Navarro, E.: Feeding and digestion by the mussel *Mytilus edulis* L. (*Bivalvia*: *Mollusca*) in mixtures of silt and algal cells at low concentrations, *J. Exp. Mar. Bio. Ecol.*, 111(1), 1–22, doi:10.1016/0022-0981(87)90017-7, 1987.
- Béjaoui-Omri, A., Béjaoui, B., Harzallah, A., Aloui-Béjaoui, N., El Bour, M. and Aleya, L.: Dynamic energy budget model: a monitoring tool for growth and reproduction performance of *Mytilus galloprovincialis* in Bizerte Lagoon (Southwestern Mediterranean Sea), *Environ. Sci. Pollut. Res.*, 21(22), 13081–13094, doi:10.1007/s11356-014-3265-1, 2014.
- Beyer, J., Green, N. W., Brooks, S., Allan, I. J., Ruus, A., Gomes, T., Bråte, I. L. N. and Schøyen, M.: Blue mussels (*Mytilus edulis* spp.) as sentinel organisms in coastal pollution monitoring: A review, *Mar. Environ. Res.*, 130, 338–365, doi:10.1016/j.marenvres.2017.07.024, 2017.
- Birnstiel, S., Soares-Gomes, A. and da Gama, B. A. P.: Depuration reduces microplastic content in wild and farmed mussels, *Mar. Pollut. Bull.*, 140, 241–247, doi:10.1016/j.marpolbul.2019.01.044, 2019.
- Bourlès, Y., Alunno-Bruscia, M., Pouvreau, S., Tollu, G., Leguay, D., Arnaud, C., Goulletquer, P. and Kooijman, S. A. L. M.: Modelling growth and reproduction of the Pacific oyster *Crassostrea gigas*: Advances in the oyster-DEB model through application to a coastal pond, *J. Sea Res.*, 62(2–3), 62–71, doi:10.1016/j.seares.2009.03.002, 2009.
- Bråte, I. L. N., Hurley, R., Iversen, K., Beyer, J., Thomas, K. V., Steindal, C. C., Green, N. W., Olsen, M. and Lusher, A.: *Mytilus* spp. as sentinels for monitoring microplastic pollution in Norwegian coastal waters: A qualitative and quantitative study, *Environ. Pollut.*, 243, 383–393, doi:10.1016/j.envpol.2018.08.077, 2018.
- Browne, M. A., Dissanayake, A., Galloway, T. S., Lowe, D. M. and Thompson, R. C.: Ingested microscopic plastic translocates to the circulatory system of the mussel, *Mytilus edulis* (L.), *Environ. Sci. Technol.*, 42(13), 5026–5031, doi:10.1021/es800249a, 2008.
- Browne, M. A., Galloway, T. and Thompson, R.: Microplastic—an emerging contaminant of potential concern?, *Integr. Environ. Assess. Manag.*, 3(4), 559–561, doi:10.1002/ieam.5630030412, 2007.
- Browne, M. A.: Sources and pathways of microplastics to habitats, *Mar. Anthropog. Litter*, 229–244, doi:10.1007/978-3-319-16510-3_9, 2015.
- Capolupo, M., Franzellitti, S., Valbonesi, P., Lanzas, C. S. and Fabbri, E.: Uptake and transcriptional effects of polystyrene microplastics in larval stages of the Mediterranean mussel *Mytilus galloprovincialis*, *Environ. Pollut.*, 241, 1038–1047, doi:10.1016/j.envpol.2018.06.035, 2018.
- Cardoso, J. F. M. F., Dekker, R., Witte, J. I. J. and van der Veer, H. W.: Is reproductive failure responsible for reduced recruitment of intertidal *Mytilus edulis* L. in the western Dutch Wadden Sea?, *Senckenbergiana Maritima*, 37(2), 83–92, doi:10.1007/BF03043695, 2007.
- Casas, S. and Bacher, C.: Modelling trace metal (Hg and Pb) bioaccumulation in the Mediterranean mussel, *Mytilus galloprovincialis*, applied to environmental monitoring, *J. Sea Res.*, 56(2), 168–181, doi:10.1016/j.seares.2006.03.006, 2006.
- Ciavatta, S., Kay, S., Brewin, R. J. W., Cox, R., Di Cicco, A., Nencioli, F., Polimene, L., Sammartino, M., Santoleri, R., Skákala, J. and Tsapakis, M.: Ecoregions in the Mediterranean Sea Through the Reanalysis of



- 856 Phytoplankton Functional Types and Carbon Fluxes, *J. Geophys. Res. Ocean.*, 124(10), 6737–6759,
 857 doi:10.1029/2019JC015128, 2019.
- 858 Cole, M., Lindeque, P., Fileman, E., Halsband, C., Goodhead, R., Moger, J. and Galloway, T. S.: Microplastic
 859 ingestion by zooplankton, *Environ. Sci. Technol.*, 47(12), 6646–6655, doi:10.1021/es400663f, 2013.
- 860 Cole, M., Lindeque, P., Halsband, C. and Galloway, T. S.: Microplastics as contaminants in the marine
 861 environment: A review, *Mar. Pollut. Bull.*, 62(12), 2588–2597, doi:10.1016/j.marpolbul.2011.09.025, 2011.
- 862 Cucci, T. L., Shumway, S. E., Brown, W. S. and Newell, C. R.: Using phytoplankton and flow cytometry to
 863 analyze grazing by marine organisms, *Cytometry*, 10(5), 659–669, doi:10.1002/cyto.990100523, 1989.
- 864 Daewel, U., Peck, M. A., Kühn, W., St. John, M. A., Alekseeva, I. and Schrum, C.: Coupling ecosystem and
 865 individual-based models to simulate the influence of environmental variability on potential growth and survival of
 866 larval sprat (*Sprattus sprattus* L.) in the North Sea, *Fish. Oceanogr.*, 17(5), 333–351, doi:10.1111/j.1365-
 867 2419.2008.00482.x, 2008.
- 868 de Sá, L. C., Oliveira, M., Ribeiro, F., Rocha, T. L. and Futter, M. N.: Studies of the effects of microplastics on
 869 aquatic organisms: What do we know and where should we focus our efforts in the future?, *Sci. Total Environ.*, 645,
 870 1029–1039, doi:10.1016/j.scitotenv.2018.07.207, 2018.
- 871 De Witte, B., Devriese, L., Bekaert, K., Hoffman, S., Vandermeersch, G., Cooreman, K. and Robbens, J.: Quality
 872 assessment of the blue mussel (*Mytilus edulis*): Comparison between commercial and wild types, *Mar. Pollut. Bull.*,
 873 85(1), 146–155, doi:10.1016/j.marpolbul.2014.06.006, 2014.
- 874 Digka, N., Tsangaris, C., Kaberi, H., Adamopoulou, A. and Zeri, C.: Microplastic Abundance and Polymer
 875 Types in a Mediterranean Environment, *Springer Water.*, 2018b.
- 876 Digka, N., Tsangaris, C., Torre, M., Anastasopoulou, A. and Zeri, C.: Microplastics in mussels and fish from the
 877 Northern Ionian Sea, *Mar. Pollut. Bull.*, 135, 30–40, doi:10.1016/j.marpolbul.2018.06.063, 2018a.
- 878 Enders, K., Lenz, R., Stedmon, C. A. and Nielsen, T. G.: Abundance, size and polymer composition of marine
 879 microplastics $\geq 10 \mu\text{m}$ in the Atlantic Ocean and their modelled vertical distribution, *Mar. Pollut. Bull.*, 100(1), 70–81,
 880 doi:10.1016/j.marpolbul.2015.09.027, 2015.
- 881 Eriksen, M., Lebreton, L. C. M., Carson, H. S., Thiel, M., Moore, C. J., Borerro, J. C., Galgani, F., Ryan, P. G.
 882 and Reisser, J.: Plastic Pollution in the World's Oceans: More than 5 Trillion Plastic Pieces Weighing over 250,000
 883 Tons Afloat at Sea, *PLoS One*, 9(12), doi:10.1371/journal.pone.0111913, 2014.
- 884 Everaert, G., Van Cauwenberghe, L., De Rijcke, M., Koelmans, A. A., Mees, J., Vandegehuchte, M. and Janssen,
 885 C. R.: Risk assessment of microplastics in the ocean: Modelling approach and first conclusions, *Environ. Pollut.*, 242,
 886 1930–1938, doi:10.1016/j.envpol.2018.07.069, 2018.
- 887 Fossi, M. C., Pedà, C., Compà, M., Tsangaris, C., Alomar, C., Claro, F., Ioakeimidis, C., Galgani, F., Hema, T.,
 888 Deudero, S., Romeo, T., Battaglia, P., Andaloro, F., Caliani, I., Casini, S., Panti, C. and Baini, M.: Bioindicators for
 889 monitoring marine litter ingestion and its impacts on Mediterranean biodiversity, *Environ. Pollut.*, 237, 1023–1040,
 890 doi:10.1016/j.envpol.2017.11.019, 2018.
- 891 Gardon, T., Reisser, C., Soyez, C., Quillien, V. and Le Moullac, G.: Microplastics Affect Energy Balance and
 892 Gametogenesis in the Pearl Oyster *Pinctada margaritifera*, *Environ. Sci. Technol.*, 52(9), 5277–5286,
 893 doi:10.1021/acs.est.8b00168, 2018.
- 894 GESAMP Joint Group of Experts on the Scientific Aspects of Marine Environmental Protection: Sources, fate
 895 and effects of microplastics in the marine environment: a global assessment”, edited by P. J. Kershaw and ed), *Reports*
 896 *Stud. GESAMP*, 90(90), 96, doi:10.13140/RG.2.1.3803.7925, 2015.
- 897 *GlobColour data (<http://globcolour.info>) used in this study has been developed, validated, and distributed by*
 898 *ACRI-ST, France.*
- 899 Gohin, F., Druon, J. N. and Lampert, L.: A five channel chlorophyll concentration algorithm applied to Sea
 900 WiFS data processed by SeaDAS in coastal waters, *Int. J. Remote Sens.*, 23(8), 1639–1661,
 901 doi:10.1080/01431160110071879, 2002.
- 902 Goldstein, M. C., Titmus, A. J. and Ford, M.: Scales of spatial heterogeneity of plastic marine debris in the
 903 northeast Pacific Ocean, *PLoS One*, 8(11), 80020, doi:10.1371/journal.pone.0080020, 2013.
- 904 Handå, A., Alver, M., Edvardsen, C. V., Halstensen, S., Olsen, A. J., Øie, G., Reitan, K. I., Olsen, Y. and
 905 Reinertsen, H.: Growth of farmed blue mussels (*Mytilus edulis* L.) in a Norwegian coastal area; comparison of food
 906 proxies by DEB modeling, *J. Sea Res.*, 66(4), 297–307, doi:10.1016/j.seares.2011.05.005, 2011.
- 907 Hantoro, I., Löhr, A. J., Van Belleghem, F. G. A. J., Widianarko, B. and Ragas, A. M. J.: Microplastics in coastal
 908 areas and seafood: implications for food safety, *Food Addit. Contam. - Part A Chem. Anal. Control. Expo. Risk*
 909 *Assess.*, 36(5), 674–711, doi:10.1080/19440049.2019.1585581, 2019.



- 110 Hatzonikolakis, Y., Tsiaras, K., Theodorou, J. A., Petihakis, G., Sofianos, S. and Triantafyllou, G.: Simulation of
- 111 mussel *Mytilus galloprovincialis* growth with a dynamic energy budget model in Maliakos and Thermaikos Gulfs
- 112 (Eastern mediterranean), *Aquac. Environ. Interact.*, 9, 371–383, doi:10.3354/aei00236, 2017.
- 113 Hirai, H., Takada, H., Ogata, Y., Yamashita, R., Mizukawa, K., Saha, M., Kwan, C., Moore, C., Gray, H.,
- 114 Laursen, D., Zettler, E. R., Farrington, J. W., Reddy, C. M., Peacock, E. E. and Ward, M. W.: Organic micropollutants
- 115 in marine plastics debris from the open ocean and remote and urban beaches, *Mar. Pollut. Bull.*, 62(8), 1683–1692,
- 116 doi:10.1016/j.marpolbul.2011.06.004, 2011.
- 117 Jacobs, P., Beauchemin, C. and Riegman, R.: Growth of juvenile blue mussels (*Mytilus edulis*) on suspended
- 118 collectors in the Dutch Wadden Sea, *J. Sea Res.*, 85, 365–371, doi:10.1016/j.seares.2013.07.006, 2014.
- 119 Jacobs, P., Troost, K., Riegman, R. and van der Meer, J.: Length- and weight-dependent clearance rates of
- 120 juvenile mussels (*Mytilus edulis*) on various planktonic prey items, *Helgol. Mar. Res.*, 69(1), 101–112,
- 121 doi:10.1007/s10152-014-0419-y, 2015.
- 122 Jolliff, J. K., Kindle, J. C., Shulman, I., Penta, B., Friedrichs, M. A. M., Helber, R. and Arnone, R. A.: Summary
- 123 diagrams for coupled hydrodynamic-ecosystem model skill assessment, *J. Mar. Syst.*, 76(1–2), 64–82,
- 124 doi:10.1016/j.jmarsys.2008.05.014, 2009.
- 125 Jørgensen, C., Larsen, P. and Riisgård, H.: Effects of temperature on the mussel pump, *Mar. Ecol. Prog. Ser.*,
- 126 64(1/2), 89–97, doi:10.3354/meps064089, 1990.
- 127 Kalaroni S, Hatzonikolakis Y, Tsiaras K, Gkanasos A, Triantafyllou G.: Modelling the Marine Microplastic
- 128 Distribution from Municipal Wastewater in Saronikos Gulf (E. Mediterranean). *Oceanogr Fish Open Access J.*; 9(1):
- 129 555752. DOI: 10.19080/OFOAJ.2019.09.555752, 2019.
- 130 Kalaroni, S., Tsiaras, K., Petihakis, G., Economou-Amilli, A. and Triantafyllou, G.: Modelling the
- 131 Mediterranean pelagic ecosystem using the POSEIDON ecological model. Part I: Nutrients and chlorophyll-a
- 132 dynamics, *Deep. Res. Part II Top. Stud. Oceanogr.*, 171, 104647, doi:10.1016/j.dsr2.2019.104647, 2020.
- 133 Karayücel, S., Çelik, M. Y., Karayücel, I. and Erik, G.: Karadeniz’de Sinop İlinde Akdeniz Midyesinin (*Mytilus*
- 134 *galloprovincialis* Lamarck, 1819) Sal Sisteminde Büyümesi ve Üretimi, *Turkish J. Fish. Aquat. Sci.*, 10(1), 9–17,
- 135 doi:10.4194/trjfas.2010.0102, 2010.
- 136 Karlsson, T. M., Vethaak, A. D., Almroth, B. C., Ariese, F., van Velzen, M., Hassellöv, M. and Leslie, H. A.:
- 137 Screening for microplastics in sediment, water, marine invertebrates and fish: Method development and microplastic
- 138 accumulation, *Mar. Pollut. Bull.*, 122(1–2), 403–408, doi:10.1016/j.marpolbul.2017.06.081, 2017.
- 139 Kearney, M., Simpson, S. J., Raubenheimer, D. and Helmuth, B.: Modelling the ecological niche from functional
- 140 traits, *Philos. Trans. R. Soc. B Biol. Sci.*, 365(1557), 3469–3483, doi:10.1098/rstb.2010.0034, 2010.
- 141 Khan, M. B. and Prezant, R. S.: Microplastic abundances in a mussel bed and ingestion by the ribbed marsh
- 142 mussel *Geukensia demissa*, *Mar. Pollut. Bull.*, 130, 67–75, doi:10.1016/j.marpolbul.2018.03.012, 2018.
- 143 Kiørboe, T. and Møhlenberg, F.: Particle Selection in Suspension-Feeding Bivalves, *Mar. Ecol. Prog. Ser.*, 5,
- 144 291–296, doi:10.3354/meps005291, 1981.
- 145 Kooi, M., Reisser, J., Slat, B., Ferrari, F. F., Schmid, M. S., Cunsolo, S., Brambini, R., Noble, K., Sirks, L. A.,
- 146 Linders, T. E. W., Schoeneich-Argent, R. I. and Koelmans, A. A.: The effect of particle properties on the depth profile
- 147 of buoyant plastics in the ocean, *Sci. Rep.*, 6(1), doi:10.1038/srep33882, 2016.
- 148 Kooijman SALM: *Dynamic Energy Budget Theory for Metabolic Organisation*. Cambridge University Press,
- 149 Cambridge, 2010.
- 150 Kooijman, S. A. L. M.: *Dynamic Energy and Mass Budgets in Biological Systems*. Cambridge: Cambridge
- 151 University Press, 2000.
- 152 Kooijman, S. A. L. M.: Pseudo-faeces production in bivalves, *J. Sea Res.*, 56(2), 103–106,
- 153 doi:10.1016/j.seares.2006.03.003, 2006.
- 154 Lacroix, G., Ruddick, K., Ozer, J. and Lancelot, C.: Modelling the impact of the Scheldt and Rhine/Meuse
- 155 plumes on the salinity distribution in Belgian waters (southern North Sea), *J. Sea Res.*, 52(3), 149–163,
- 156 doi:10.1016/j.seares.2004.01.003, 2004.
- 157 Lattin, G. L., Moore, C. J., Zellers, A. F., Moore, S. L. and Weisberg, S. B.: A comparison of neustonic plastic
- 158 and zooplankton at different depths near the southern California shore, *Mar. Pollut. Bull.*, 49(4), 291–294,
- 159 doi:10.1016/j.marpolbul.2004.01.020, 2004.
- 160 Law, K. L. and Thompson, R. C.: Microplastics in the seas, *Science* (80-.), 345(6193), 144–145,
- 161 doi:10.1126/science.1254065, 2014.
- 162 Lenz, R., Enders, K. and Nielsen, T. G.: Microplastic exposure studies should be environmentally realistic, *Proc.*
- 163 *Natl. Acad. Sci. U. S. A.*, 113(29), E4121–E4122, doi:10.1073/pnas.1606615113, 2016.



- 964 Li, J., Green, C., Reynolds, A., Shi, H. and Rotchell, J. M.: Microplastics in mussels sampled from coastal waters
 965 and supermarkets in the United Kingdom, *Environ. Pollut.*, 241, 35–44, doi:10.1016/j.envpol.2018.05.038, 2018.
- 966 Li, J., Lusher, A. L., Rotchell, J. M., Deudero, S., Turra, A., Bråte, I. L. N., Sun, C., Shahadat Hossain, M., Li,
 967 Q., Kolandhasamy, P. and Shi, H.: Using mussel as a global bioindicator of coastal microplastic pollution, *Environ.*
 968 *Pollut.*, 244, 522–533, doi:10.1016/j.envpol.2018.10.032, 2019.
- 969 Li, J., Qu, X., Su, L., Zhang, W., Yang, D., Kolandhasamy, P., Li, D. and Shi, H.: Microplastics in mussels along
 970 the coastal waters of China, *Environ. Pollut.*, 214, 177–184, doi:10.1016/j.envpol.2016.04.012, 2016.
- 971 Liubartseva, S., Coppini, G., Lecci, R. and Clementi, E.: Tracking plastics in the Mediterranean: 2D Lagrangian
 972 model, *Mar. Pollut. Bull.*, 129(1), 151–162, doi:10.1016/j.marpolbul.2018.02.019, 2018.
- 973 Lusher, A., Bråte, I. L. N., Hurley, R., Iversen, K. and Olsen, M.: Testing of methodology for measuring
 974 microplastics in blue mussels (*Mytilus* spp) and sediments, and recommendations for future monitoring of
 975 microplastics, 87, (7209), doi:10.13140/RG.2.2.24399.59041, 2017.
- 976 Lusher, A.: Microplastics in the marine environment: Distribution, interactions and effects, *Mar. Anthropog.*
 977 *Litter*, 245–307, doi:10.1007/978-3-319-16510-3_10, 2015.
- 978 Maes, T., Van der Meulen, M. D., Devriese, L. I., Leslie, H. A., Huvet, A., Frère, L., Robbens, J. and Vethaak,
 979 A. D.: Microplastics baseline surveys at the water surface and in sediments of the North-East Atlantic, *Front. Mar.*
 980 *Sci.*, 4(MAY), doi:10.3389/fmars.2017.00135, 2017.
- 981 Maire, O., Amouroux, J. M., Duchêne, J. C. and Grémare, A.: Relationship between filtration activity and food
 982 availability in the Mediterranean mussel *Mytilus galloprovincialis*, *Mar. Biol.*, 152(6), 1293–1307,
 983 doi:10.1007/s00227-007-0778-x, 2007.
- 984 MarLIN: The Marine Life Information Network - Common mussel (*Mytilus edulis*). Available from:
 985 <https://www.marlin.ac.uk/species/detail/1421>, 2016.
- 986 Mathalon, A. and Hill, P.: Microplastic fibers in the intertidal ecosystem surrounding Halifax Harbor, Nova
 987 Scotia, *Mar. Pollut. Bull.*, 81(1), 69–79, doi:10.1016/j.marpolbul.2014.02.018, 2014.
- 988 Mato, Y., Isobe, T., Takada, H., Kanehiro, H., Ohtake, C. and Kaminuma, T.: Plastic resin pellets as a transport
 989 medium for toxic chemicals in the marine environment, *Environ. Sci. Technol.*, 35(2), 318–324,
 990 doi:10.1021/es0010498, 2001.
- 991 Messinetti, S., Mercurio, S., Parolini, M., Sugni, M. and Pennati, R.: Effects of polystyrene microplastics on
 992 early stages of two marine invertebrates with different feeding strategies, *Environ. Pollut.*, 237, 1080–1087,
 993 doi:10.1016/j.envpol.2017.11.030, 2018.
- 994 Monaco, C. J. and McQuaid, C. D.: Applicability of Dynamic Energy Budget (DEB) models across steep
 995 environmental gradients, *Sci. Rep.*, 8(1), doi:10.1038/s41598-018-34786-w, 2018.
- 996 Moore, C. J., Moore, S. L., Leecaster, M. K. and Weisberg, S. B.: A comparison of plastic and plankton in the
 997 North Pacific Central Gyre, *Mar. Pollut. Bull.*, 42(12), 1297–1300, doi:10.1016/S0025-326X(01)00114-X, 2001.
- 998 Otto, L., Zimmerman, J. T. F., Furnes, G. K., Mork, M., Saetre, R. and Becker, G.: Review of the physical
 999 oceanography of the North Sea, *Netherlands J. Sea Res.*, 26(2–4), 161, doi:10.1016/0077-7579(90)90091-T, 1990.
- 1000 Painting, S. J., Collingridge, K. A., Durand, D., Grémare, A., Créach, V., Arvanitidis, C. and Bernard, G.:
 1001 Marine monitoring in Europe: is it adequate to address environmental threats and pressures?, *Ocean Sci. Discuss.*,
 1002 16(1), 1–31, doi:10.5194/os-2019-75, 2019.
- 1003 Palacz, A. P., St. John, M. A., Brewin, R. J. W., Hirata, T. and Gregg, W. W.: Distribution of phytoplankton
 1004 functional types in high-nitrate, low-chlorophyll waters in a new diagnostic ecological indicator model,
 1005 *Biogeosciences*, 10(11), 7553–7574, doi:10.5194/bg-10-7553-2013, 2013.
- 1006 Pascoe, P. L., Parry, H. E. and Hawkins, A. J. S.: Observations on the measurement and interpretation of
 1007 clearance rate variations in suspension-feeding bivalve shellfish, *Aquat. Biol.*, 6(1–3), 181–190, doi:10.3354/ab00123,
 1008 2009.
- 1009 Pasquini, G., Ronchi, F., Strafella, P., Scarcella, G. and Fortibuoni, T.: Seabed litter composition, distribution
 1010 and sources in the Northern and Central Adriatic Sea (Mediterranean), *Waste Manag.*, 58, 41–51,
 1011 doi:10.1016/j.wasman.2016.08.038, 2016.
- 1012 Petihakis, G., Triantafyllou, G., Allen, I. J., Hoteit, I. and Dounas, C.: Modelling the spatial and temporal
 1013 variability of the Cretan Sea ecosystem, *J. Mar. Syst.*, 36(3–4), 173–196, doi:10.1016/S0924-7963(02)00186-0, 2002.
- 1014 Petihakis, G., Triantafyllou, G., Korres, G., Tsiaras, K. and Theodorou, A.: Ecosystem modelling: Towards the
 1015 development of a management tool for a marine coastal system part-II, ecosystem processes and biogeochemical
 1016 fluxes, *J. Mar. Syst.*, 94(SUPPL.), 49– 64, doi:10.1016/j.jmarsys.2011.11.006, 2012.



- 1017 Politikos, D. V., Tsiaras, K., Papatheodorou, G. and Anastasopoulou, A.: Modeling of floating marine litter
1018 originated from the Eastern Ionian Sea: Transport, residence time and connectivity, *Mar. Pollut. Bull.*, 150, 110727,
1019 doi:10.1016/j.marpolbul.2019.110727, 2020.
- 1020 Pouvreau, S., Bourles, Y., Lefebvre, S., Gangnery, A. and Alunno-Bruscia, M.: Application of a dynamic energy
1021 budget model to the Pacific oyster, *Crassostrea gigas*, reared under various environmental conditions, *J. Sea Res.*,
1022 56(2), 156–167, doi:10.1016/j.seares.2006.03.007, 2006.
- 1023 Prins, T. C., Smaal, A. C. and Pouwer, A. J.: Selective ingestion of phytoplankton by the bivalves *Mytilus edulis*
1024 L. and *Cerastoderma edule* (L.), *Hydrobiol. Bull.*, 25(1), 93–100, doi:10.1007/BF02259595, 1991.
- 1025 Qu, X., Su, L., Li, H., Liang, M. and Shi, H.: Assessing the relationship between the abundance and properties of
1026 microplastics in water and in mussels, *Sci. Total Environ.*, 621, 679–686, doi:10.1016/j.scitotenv.2017.11.284, 2018.
- 1027 Raitsos, D. E., Korres, G., Triantafyllou, G., Petihakis, G., Pantazi, M., Tsiaras, K. and Pollani, A.: Assessing
1028 chlorophyll variability in relation to the environmental regime in Pagasitikos Gulf, Greece, *J. Mar. Syst.*, 94(SUPPL.),
1029 16–22, doi:10.1016/j.jmarsys.2011.11.003, 2012.
- 1030 Raitsos, D. E., Lavender, S. J., Maravelias, C. D., Haralabous, J., Richardson, A. J. and Reid, P. C.: Identifying
1031 four phytoplankton functional types from space: An ecological approach, *Limnol. Oceanogr.*, 53(2), 605–613,
1032 doi:10.4319/lo.2008.53.2.0605, 2008.
- 1033 Raitsos, D. E., Pradhan, Y., Lavender, S. J., Hoteit, I., Mcquatters-Gollop, A., Reid, P. C. and Richardson, A. J.:
1034 From silk to satellite: Half a century of ocean colour anomalies in the Northeast Atlantic, *Glob. Chang. Biol.*, 20(7),
1035 2117–2123, doi:10.1111/gcb.12457, 2014.
- 1036 Raitsos, D. E., Reid, P. C., Lavender, S. J., Edwards, M. and Richardson, A. J.: Extending the SeaWiFS
1037 chlorophyll data set back 50 years in the northeast Atlantic, *Geophys. Res. Lett.*, 32(6), 1–4,
1038 doi:10.1029/2005GL022484, 2005.
- 1039 Ren, J. S.: Effect of food quality on energy uptake, *J. Sea Res.*, 62(2–3), 72–74,
1040 doi:10.1016/j.seares.2008.11.002, 2009.
- 1041 Riisgård, H. U., Egede, P. P. and Barreiro Saavedra, I.: Feeding Behaviour of the Mussel, *Mytilus edulis* : New
1042 Observations, with a Minireview of Current Knowledge , *J. Mar. Biol.*, 2011, 1–13, doi:10.1155/2011/312459, 2011.
- 1043 Riisgård, H. U., Kittner, C. and Seerup, D. F.: Regulation of opening state and filtration rate in filter-feeding
1044 bivalves (*Cardium edule*, *Mytilus edulis*, *Mya arenaria*) in response to low algal concentration, *J. Exp. Mar. Bio. Ecol.*,
1045 284(1–2), 105–127, doi:10.1016/S0022-0981(02)00496-3, 2003.
- 1046 Rios, L. M., Moore, C. and Jones, P. R.: Persistent organic pollutants carried by synthetic polymers in the ocean
1047 environment, *Mar. Pollut. Bull.*, 54(8), 1230–1237, doi:10.1016/j.marpolbul.2007.03.022, 2007.
- 1048 Rist, S., Steensgaard, I. M., Guven, O., Nielsen, T. G., Jensen, L. H., Møller, L. F. and Hartmann, N. B.: The fate
1049 of microplastics during uptake and depuration phases in a blue mussel exposure system, *Environ. Toxicol. Chem.*,
1050 38(1), 99–105, doi:10.1002/etc.4285, 2019.
- 1051 Romeo, T., Pietro, B., Pedà, C., Consoli, P., Andaloro, F. and Fossi, M. C.: First evidence of presence of plastic
1052 debris in stomach of large pelagic fish in the Mediterranean Sea, *Mar. Pollut. Bull.*, 95(1), 358–361,
1053 doi:10.1016/j.marpolbul.2015.04.048, 2015.
- 1054 Rosland, R., Strand, Alunno-Bruscia, M., Bacher, C. and Strohmeier, T.: Applying Dynamic Energy Budget
1055 (DEB) theory to simulate growth and bio-energetics of blue mussels under low seston conditions, *J. Sea Res.*, 62(2–3),
1056 49–61, doi:10.1016/j.seares.2009.02.007, 2009.
- 1057 Santana, M. F. M., Moreira, F. T., Pereira, C. D. S., Abessa, D. M. S. and Turra, A.: Continuous Exposure to
1058 Microplastics Does Not Cause Physiological Effects in the Cultivated Mussel *Perna perna*, *Arch. Environ. Contam.*
1059 *Toxicol.*, 74(4), 594–604, doi:10.1007/s00244-018-0504-3, 2018.
- 1060 Sarà, G., Kearney, M. and Helmuth, B.: Combining heat-transfer and energy budget models to predict thermal
1061 stress in Mediterranean intertidal mussels, *Chem. Ecol.*, 27(2), 135–145, doi:10.1080/02757540.2011.552227, 2011.
- 1062 Sarà, G., Milanese, M., Prusina, I., Sarà, A., Angel, D. L., Glamuzina, B., Nitzan, T., Freeman, S., Rinaldi, A.,
1063 Palmeri, V., Montalto, V., Lo Martire, M., Gianguzza, P., Arizza, V., Lo Brutto, S., De Pirro, M., Helmuth, B.,
1064 Murray, J., De Cantis, S. and Williams, G. A.: The impact of climate change on mediterranean intertidal communities:
1065 Losses in coastal ecosystem integrity and services, *Reg. Environ. Chang.*, 14(SUPPL.1), 5–17, doi:10.1007/s10113-
1066 012-0360-z, 2014.
- 1067 Sarà, G., Reid, G. K., Rinaldi, A., Palmeri, V., Troell, M. and Kooijman, S. A. L. M.: Growth and reproductive
1068 simulation of candidate shellfish species at fish cages in the Southern Mediterranean: Dynamic Energy Budget (DEB)
1069 modelling for integrated multi-trophic aquaculture, *Aquaculture*, 324–325, 259–266,
1070 doi:10.1016/j.aquaculture.2011.10.042, 2012.



- 1071 Saraiva, S., der Meer, J. van, Kooijman, S. A. L. M. and Sousa, T.: DEB parameters estimation for *Mytilus*
- 1072 *edulis*, J. Sea Res., 66(4), 289–296, doi:10.1016/j.seares.2011.06.002, 2011b.
- 1073 Saraiva, S., van der Meer, J., Kooijman, S. A. L. M. and Sousa, T.: Modelling feeding processes in bivalves: A
- 1074 mechanistic approach, Ecol. Modell., 222(3), 514–523, doi:10.1016/j.ecolmodel.2010.09.031, 2011a.
- 1075 Saraiva, S., Van Der Meer, J., Kooijman, S. A. L. M., Witbaard, R., Philippart, C. J. M., Hippler, D. and Parker,
- 1076 R.: Validation of a Dynamic Energy Budget (DEB) model for the blue mussel *Mytilus edulis*, Mar. Ecol. Prog. Ser.,
- 1077 463, 141–158, doi:10.3354/meps09801, 2012.
- 1078 Schwabl, P., Koppel, S., Königshofer, P., Bucsics, T., Trauner, M., Reiberger, T. and Liebmann, B.: Detection of
- 1079 various microplastics in human stool: A prospective case series, Ann. Intern. Med., 171(7), 453–457,
- 1080 doi:10.7326/M19-0618, 2019.
- 1081 Seuront, L., Nicastro, K. R., Zardi, G. I. and Goberville, E.: Decreased thermal tolerance under recurrent heat
- 1082 stress conditions explains summer mass mortality of the blue mussel *Mytilus edulis*, Sci. Rep., 9(1),
- 1083 doi:10.1038/s41598-019-53580-w, 2019.
- 1084 Skoulidakis, N. T., Economou, A. N., Gritsalis, K. C. and Zogaris, S.: Rivers of the Balkans, Rivers Eur., 421–
- 1085 466, doi:10.1016/B978-0-12-369449-2.00011-4, 2009.
- 1086 Smith, M., Love, D. C., Rochman, C. M. and Neff, R. A.: Microplastics in Seafood and the Implications for
- 1087 Human Health, Curr. Environ. Heal. reports, 5(3), 375–386, doi:10.1007/s40572-018-0206-z, 2018.
- 1088 Sprung, M.: Reproduction and fecundity of the mussel *mytilus edulis* at helgoland (North sea), Helgoländer
- 1089 Meeresuntersuchungen, 36(3), 243–255, doi:10.1007/BF01983629, 1983.
- 1090 Sukhotin, A. A. and Kulakowski, E. E.: Growth and population dynamics in mussels (*Mytilus edulis* L.) cultured
- 1091 in the White Sea, Aquaculture, 101(1–2), 59–73, doi:10.1016/0044-8486(92)90232-A, 1992.
- 1092 Sukhotin, A. A., Strelkov, P. P., Maximovich, N. V. and Hummel, H.: Growth and longevity of *Mytilus edulis*
- 1093 (L.) from northeast Europe, Mar. Biol. Res., 3(3), 155–167, doi:10.1080/17451000701364869, 2007.
- 1094 Sussarellu, R., Suquet, M., Thomas, Y., Lambert, C., Fabioux, C., Pernet, M. E. J., Goic, N. Le, Quillien, V.,
- 1095 Mingant, C., Epelboin, Y., Corporeau, C., Guyomarch, J., Robbens, J., Paul-Pont, I., Soudant, P. and Huvet, A.: Oyster
- 1096 reproduction is affected by exposure to polystyrene microplastics, Proc. Natl. Acad. Sci. U. S. A., 113(9), 2430–2435,
- 1097 doi:10.1073/pnas.1519019113, 2016.
- 1098 Tagliarolo, M. and McQuaid, C. D.: Sub-lethal and sub-specific temperature effects are better predictors of
- 1099 mussel distribution than thermal tolerance, Mar. Ecol. Prog. Ser., 535, 145–159, doi:10.3354/meps11434, 2015.
- 1100 Teuten, E. L., Rowland, S. J., Galloway, T. S. and Thompson, R. C.: Potential for plastics to transport
- 1101 hydrophobic contaminants, Environ. Sci. Technol., 41(22), 7759–7764, doi:10.1021/es071737s, 2007.
- 1102 Teuten, E. L., Saquing, J. M., Knappe, D. R. U., Barlaz, M. A., Jonsson, S., Björn, A., Rowland, S. J.,
- 1103 Thompson, R. C., Galloway, T. S., Yamashita, R., Ochi, D., Watanuki, Y., Moore, C., Viet, P. H., Tana, T. S.,
- 1104 Prudente, M., Boonyatumanond, R., Zakaria, M. P., Akkhavong, K., Ogata, Y., Hirai, H., Iwasa, S., Mizukawa, K.,
- 1105 Hagino, Y., Imamura, A., Saha, M. and Takada, H.: Transport and release of chemicals from plastics to the
- 1106 environment and to wildlife, Philos. Trans. R. Soc. B Biol. Sci., 364(1526), 2027–2045, doi:10.1098/rstb.2008.0284,
- 1107 2009.
- 1108 Theodorou, J. A., Viaene, J., Sorgeloos, P. and Tzovenis, I.: Production and Marketing Trends of the Cultured
- 1109 Mediterranean Mussel *Mytilus galloprovincialis* Lamarck 1819, in Greece , J. Shellfish Res., 30(3), 859–874,
- 1110 doi:10.2983/035.030.0327, 2011.
- 1111 Thomas, Y., Mazurić, J., Alunno-Bruscia, M., Bacher, C., Bouget, J. F., Gohin, F., Pouvreau, S. and Struski, C.:
- 1112 Modelling spatio-temporal variability of *Mytilus edulis* (L.) growth by forcing a dynamic energy budget model with
- 1113 satellite-derived environmental data, J. Sea Res., 66(4), 308–317, doi:10.1016/j.seares.2011.04.015, 2011.
- 1114 Thompson, R. C., Olson, Y., Mitchell, R. P., Davis, A., Rowland, S. J., John, A. W. G., McGonigle, D. and
- 1115 Russell, A. E.: Lost at Sea: Where Is All the Plastic?, Science (80-.), 304(5672), 838, doi:10.1126/science.1094559,
- 1116 2004.
- 1117 Triantafyllou, G., Petihakis, G. and Allen, I. J.: Assessing the performance of the Cretan Sea ecosystem model
- 1118 with the use of high frequency M3A buoy data set, Ann. Geophys., 21(1), 365–375, doi:10.5194/angeo-21-365-2003,
- 1119 2003.
- 1120 Troost, T. A., Desclaux, T., Leslie, H. A., van Der Meulen, M. D. and Vethaak, A. D.: Do microplastics affect
- 1121 marine ecosystem productivity?, Mar. Pollut. Bull., 135, 17–29, doi:10.1016/j.marpolbul.2018.05.067, 2018.
- 1122 Troost, T. A., Wijsman, J. W. M., Saraiva, S. and Freitas, V.: Modelling shellfish growth with dynamic energy
- 1123 budget models: An application for cockles and mussels in the Oosterschelde (southwest Netherlands), Philos. Trans. R.
- 1124 Soc. B Biol. Sci., 365(1557), 3567–3577, doi:10.1098/rstb.2010.0074, 2010.



- 1125 Tsiaras, K. P., Petihakis, G., Kourafalou, V. H. and Triantafyllou, G.: Impact of the river nutrient load variability
 1126 on the North Aegean ecosystem functioning over the last decades, *J. Sea Res.*, 86, 97–109,
 1127 doi:10.1016/j.seares.2013.11.007, 2014.
- 1128 Vahl, O.: Efficiency of particle retention in *Mytilus edulis* L., *Ophelia*, 10(1), 17–25,
 1129 doi:10.1080/00785326.1972.10430098, 1972.
- 1130 van Beusekom, J. E. E., Loebl, M. and Martens, P.: Distant riverine nutrient supply and local temperature drive
 1131 the long-term phytoplankton development in a temperate coastal basin, *J. Sea Res.*, 61(1–2), 26–33,
 1132 doi:10.1016/j.seares.2008.06.005, 2009.
- 1133 Van Cauwenberghe, L. and Janssen, C. R.: Microplastics in bivalves cultured for human consumption, *Environ.*
 1134 *Pollut.*, 193, 65–70, doi:10.1016/j.envpol.2014.06.010, 2014.
- 1135 Van Cauwenberghe, L., Claessens, M., Vandegehuchte, M. B. and Janssen, C. R.: Microplastics are taken up by
 1136 mussels (*Mytilus edulis*) and lugworms (*Arenicola marina*) living in natural habitats, *Environ. Pollut.*, 199, 10–17,
 1137 doi:10.1016/j.envpol.2015.01.008, 2015.
- 1138 van der Veer, H. W., Cardoso, J. F. M. F. and van der Meer, J.: The estimation of DEB parameters for various
 1139 Northeast Atlantic bivalve species, *J. Sea Res.*, 56(2), 107–124, doi:10.1016/j.seares.2006.03.005, 2006.
- 1140 van Haren, R. J. F., Schepers, H. E. and Kooijman, S. A. L. M.: Dynamic energy budgets affect kinetics of
 1141 xenobiotics in the marine mussel *Mytilus edulis*, *Chemosphere*, 29(2), 163–189, doi:10.1016/0045-6535(94)90099-X,
 1142 1994.
- 1143 Van Sebille, E., Wilcox, C., Lebreton, L., Maximenko, N., Hardesty, B. D., Van Franeker, J. A., Eriksen, M.,
 1144 Siegel, D., Galgani, F. and Law, K. L.: A global inventory of small floating plastic debris, *Environ. Res. Lett.*, 10(12),
 1145 124006, doi:10.1088/1748-9326/10/12/124006, 2015.
- 1146 Vandermeersch, G., Lourenço, H. M., Alvarez-Muñoz, D., Cunha, S., Diogène, J., Cano-Sancho, G., Sloth, J. J.,
 1147 Kwadijk, C., Barcelo, D., Allegaert, W., Bekaert, K., Fernandes, J. O., Marques, A. and Robbens, J.: Environmental
 1148 contaminants of emerging concern in seafood - European database on contaminant levels, *Environ. Res.*, 143, 29–45,
 1149 doi:10.1016/j.envres.2015.06.011, 2015.
- 1150 Vlachogianni, T., Anastasopoulou, A., Fortibuoni, T., Ronchi, F. and Zeri, C.: Marine Litter Assessment in the
 1151 Adriatic & Ionian Seas. IPA-Adriatic DeFishGear Project, MIO-ECSDE, HCMR and ISPRA. pp. 168 (ISBN: 978-
 1152 960-6793-25-7), 2017.
- 1153 Von Moos, N., Burkhardt-Holm, P. and Köhler, A.: Uptake and effects of microplastics on cells and tissue of the
 1154 blue mussel *Mytilus edulis* L. after an experimental exposure, *Environ. Sci. Technol.*, 46(20), 11327–11335,
 1155 doi:10.1021/es302332w, 2012.
- 1156 Ward, J. E. and Kach, D. J.: Marine aggregates facilitate ingestion of nanoparticles by suspension-feeding
 1157 bivalves, *Mar. Environ. Res.*, 68(3), 137–142, doi:10.1016/j.marenvres.2009.05.002, 2009.
- 1158 Ward, J. E. and Shumway, S. E.: Separating the grain from the chaff: Particle selection in suspension- and
 1159 deposit-feeding bivalves, *J. Exp. Mar. Bio. Ecol.*, 300(1–2), 83–130, doi:10.1016/j.jembe.2004.03.002, 2004.
- 1160 Ward, J. E., Zhao, S., Holohan, B. A., Mladinich, K. M., Griffin, T. W., Wozniak, J. and Shumway, S. E.:
 1161 Selective Ingestion and Egestion of Plastic Particles by the Blue Mussel (*Mytilus edulis*) and Eastern Oyster
 1162 (*Crassostrea virginica*): Implications for Using Bivalves as Bioindicators of Microplastic Pollution, *Environ. Sci.*
 1163 *Technol.*, 53(15), 8776–8784, doi:10.1021/acs.est.9b02073, 2019.
- 1164 Wegner, A., Besseling, E., Foekema, E. M., Kamermans, P. and Koelmans, A. A.: Effects of nanoplastyrene on
 1165 the feeding behavior of the blue mussel (*Mytilus edulis* L.), *Environ. Toxicol. Chem.*, 31(11), 2490–2497,
 1166 doi:10.1002/etc.1984, 2012.
- 1167 Widdows, J., Fieth, P. and Worrall, C. M.: Relationships between seston, available food and feeding activity in
 1168 the common mussel *Mytilus edulis*, *Mar. Biol.*, 50(3), 195–207, doi:10.1007/BF00394201, 1979.
- 1169 Wieczorek, A. M., Morrison, L., Croot, P. L., Allcock, A. L., MacLoughlin, E., Savard, O., Brownlow, H. and
 1170 Doyle, T. K.: Frequency of microplastics in mesopelagic fishes from the Northwest Atlantic, *Front. Mar. Sci.*, 5(FEB),
 1171 doi:10.3389/fmars.2018.00039, 2018.
- 1172 Woods, M. N., Stack, M. E., Fields, D. M., Shaw, S. D. and Matrai, P. A.: Microplastic fiber uptake, ingestion,
 1173 and egestion rates in the blue mussel (*Mytilus edulis*), *Mar. Pollut. Bull.*, 137, 638–645,
 1174 doi:10.1016/j.marpolbul.2018.10.061, 2018.
- 1175 Zaldivar, J. M.: A general bioaccumulation DEB model for mussels. JRC Scientific and Technical Reports, EUR
 1176 23626. Office for Official Publications of the European Communities: Luxembourg, ISBN 978-92-79-10943-0 , ii, 31
 1177 pp, 2008.



1178 Zeri, C., Adamopoulou, A., Bojanić Varezić, D., Fortibuoni, T., Kovač Viršek, M., Kržan, A., Mandić, M.,
1179 Mazziotti, C., Palatinus, A., Peterlin, M., Prvan, M., Ronchi, F., Siljic, J., Tutman, P. and Vlachogianni, T.: Floating
1180 plastics in Adriatic waters (Mediterranean Sea): From the macro- to the micro-scale, Mar. Pollut. Bull., 136, 341–350,
1181 doi:10.1016/j.marpolbul.2018.09.016, 2018.

1182 Zhao, S., Ward, J. E., Danley, M. and Mincer, T. J.: Field-Based Evidence for Microplastic in Marine Aggregates
1183 and Mussels: Implications for Trophic Transfer, Environ. Sci. Technol., 52(19), 11038–11048,
1184 doi:10.1021/acs.est.8b03467, 2018.

1185

1186

1187

1188

1189

1190

1191

1192

1193

1194

1195

1196

1197

1198

1199

1200

1201

1202

1203



1204 Tables & Figures

$$1205 \quad \frac{dE}{dt} = \dot{p}_a - \dot{p}_c \quad (1)$$

$$1206 \quad \frac{dV}{dt} = \frac{k \cdot \dot{p}_c - [\dot{p}_M] \cdot V}{[E_g]} \quad (2)$$

$$1207 \quad \frac{dR}{dt} = (1 - k) \cdot \dot{p}_c - \left[\frac{1-k}{k} \right] \cdot \min(V, V_p) \cdot [\dot{p}_M] \quad (3)$$

$$1208 \quad \dot{p}_a = \{\dot{p}_{Am}\} \cdot f \cdot k(T) \cdot V^{\frac{2}{3}} \quad (4)$$

$$1209 \quad f = \frac{X}{X + K_y}, \quad \text{where } K_y = X_K \cdot \left(1 + \frac{Y}{Y_K}\right) \quad (5)$$

$$1210 \quad \dot{p}_c = \frac{[E]}{[E_g] + k \cdot [E]} \cdot \left(\frac{[E_g] \cdot \{\dot{p}_{Am}\} \cdot k(T) \cdot V^{\frac{2}{3}}}{[E_m]} + [\dot{p}_M] \cdot V \right) \quad (6)$$

$$1211 \quad [E] = \frac{E}{V} \quad (7)$$

$$1212 \quad [\dot{p}_M] = k(T) \cdot [\dot{p}_M]_m \quad (8)$$

$$1213 \quad k(T) = \frac{\exp\left(\frac{T_A - T_A}{T_I - T}\right)}{1 + \exp\left(\frac{T_{AL} - T_{AL}}{T - T_L}\right) + \exp\left(\frac{T_{AH} - T_{AH}}{T - T_H}\right)} \quad (9)$$

$$1214 \quad L = \frac{1}{\delta_m V^{\frac{1}{3}}} \quad (10)$$

$$1215 \quad W = d \cdot \left(V + \frac{E}{[E_g]} \right) + \frac{R}{\mu_E} \quad (11)$$

$$1216 \quad \dot{C}_R = \frac{\{\dot{C}_{Rm}\}}{1 + \sum_i^n \frac{X_i \cdot \{\dot{C}_{Rm}\}}{\{\dot{p}_{XiFm}\}}} \cdot k(T) \cdot V^{\frac{2}{3}}, \quad i = \begin{cases} 1 & \text{for CHL} - a \\ 2 & \text{for MPs} \end{cases} \quad (12)^a$$

$$1217 \quad \dot{p}_{XiF} = \dot{C}_R \cdot X_i \quad (13)^a$$

$$1218 \quad \dot{p}_{XiI} = \frac{\rho_{Xi} \cdot \dot{p}_{XiF}}{1 + \sum_i^n \frac{\rho_{Xi} \cdot \dot{p}_{XiF}}{\{\dot{p}_{XiIm}\}}} \quad (14)^a$$

$$1219 \quad \dot{J}_{pfi} = \dot{p}_{XiF} - \dot{p}_{XiI} \quad (15)^a$$

$$1220 \quad \dot{J}_f = \dot{p}_{X1I} - \dot{p}_A \quad (16)$$

$$1221 \quad GSI = \frac{\frac{R}{\mu_E}}{d \cdot \left(V + \frac{E}{[E_g]} \right) + \frac{R}{\mu_E}} \quad (17)$$

1222 Table 1. Dynamic energy budget model: equations. See Table 2 for model variables, Table 3 for parameters and Table
 1223 4 for initial values

1224 ^a notation refers to feeding equations handling each type of suspended matter separately ($i=1$ for algae and $i=2$ for
 1225 microplastics) where units transformation is applied when it is necessary (see Table 3).



1226

1227

1228	Variable	Description	Units
1229	V	Structural volume	cm^3
1230	E	Energy reserves	J
1231	R	Energy allocated to development	
1232		and reproduction	J
1233	C	Microplastics accumulation	particles individual ⁻¹
1234	\dot{p}_a	Assimilation energy rate	J d^{-1}
1235	\dot{p}_c	Utilization energy rate	J d^{-1}
1236	\dot{C}_R	Clearance rate	$\text{m}^3 \text{d}^{-1}$
1237	C_{env}	Microplastics concentration	particles L^{-1}
1238	\dot{p}_{XiF}	Filtration rate	J d^{-1} or g d^{-1}
1239	\dot{p}_{XiI}	Ingestion rate	J d^{-1} or g d^{-1}
1240	\dot{J}_{pfi}	Pseudofaeces production rate	J d^{-1} or g d^{-1}
1241	\dot{J}_f	Faeces production rate	J d^{-1}
1242	f	Functional response function	-
1243	X_i	Food or MPs density	mg chl a m^{-3} or g m^{-3}
1244	$[\dot{p}_M]$	Maintenance costs	$\text{J cm}^{-3} \text{d}^{-1}$
1245	T	Temperature	K
1246	$k(T)$	Temperature dependence	-
1247	L	Shell length	cm
1248	W	Fresh tissue mass	g
1249	GSI	Gonado-somatic index	-

1250

Table 2. Dynamic energy budget model: variables

1251

1252

1253



1254	Parameter	Units	Description	Value	Reference
1255	$\{p_{Am}\}$	$\text{J cm}^{-2} \text{d}^{-1}$	Maximum surface area-specific assimilation rate	147.6	Van der Veer et al. (2006)
1256	$\{c_{Rm}\}$	$\text{m}^3 \text{cm}^{-2} \text{d}^{-1}$	Maximum surface area-specific clearance rate	0.096	Saraiva et al. (2011a)
1257	$\{p_{X_1Fm}\}$	$\text{mg chl a cm}^{-2} \text{d}^{-1}$	Algal maximum surface area-specific filtration rate*	0.1152	Rosland et al. (2009)
1258	$\{p_{X_2Fm}\}$	$\text{g cm}^{-2} \text{d}^{-1}$	Silt maximum surface area-specific filtration rate	3.5	Saraiva et al. (2011a)
1259	$\{p_{X_1Im}\}$	mg chl a d^{-1}	Algae maximum ingestion rate*	$3.12 \cdot 10^6$	Saraiva et al. (2011b)
1260	$\{p_{X_2Im}\}$	g d^{-1}	Silt maximum ingestion rate	0.11	Saraiva et al. (2011b)
1261	ρ_1	-	Algae binding probability	0.99	Saraiva et al. (2011a)
1262	ρ_2	-	Inorganic material binding probability	0.45	Saraiva et al. (2011a)
1263	X_K	mg chl a m^{-3}	Half saturation coefficient	Calibrated	-
1264	T_A	K	Arrhenius temperature	5800	Van der Veer et al. (2006)
1265	T_I	K	Reference temperature	293	Van der Veer et al. (2006)
1266	T_L	K	Lower boundary of tolerance rate	275	Van der Veer et al. (2006)
1267	T_H	K	Upper boundary of tolerance rate	296	Van der Veer et al. (2006)
1268	T_{AL}	K	Rate of decrease of upper boundary	45430	Van der Veer et al. (2006)
1269	T_{AH}	K	Rate of decrease of lower boundary	31376	Van der Veer et al. (2006)
1270	$[p_M]_m$	$\text{J cm}^{-3} \text{d}^{-1}$	Volume specific maintenance costs	24	Van der Veer et al. (2006)
1271	$[E_G]$	J cm^{-3}	Volume specific growth costs	1900	Van der Veer et al. (2006)
1272	$[E_m]$	J cm^{-3}	Maximum energy density	2190	Van der Veer et al. (2006)
1273	k	-	Fraction of utilized energy spent on maintenance/growth	0.7	Van der Veer et al. (2006)
1274	V_p	cm^3	Volume at start of reproductive stage	0.06	Van der Veer et al. (2006)
1275	GSI_{th}	-	Gonado-somatic index triggering spawning	0.28	Van der Veer et al. (2006)
1276	δ_m	-	Shape coefficient	0.25	Casas & Bacher (2006)
1277	d	g cm^{-3}	Specific density	1.0	Kooijman (2000)
1278	μ_E	J g^{-1}	Energy content of reserves	6750	Casas & Bacher (2006)
1279	λ	J mg chl a^{-1}	Conversion factor	2387.73	Rosland et al. (2009)

1280 Table 3. Dynamic energy budget model: parameters

1281 *units mol C converted to mg CHL-a by multiplying with the factor $\frac{12 \cdot 10^3}{50}$ assuming Carbon:CHL-a ratio of 50
 1282 (Hatzonikolakis et al., 2017).



1283

1284

1285

Area	X_k value (mg m^{-3})	CHL-a range (mg m^{-3})	CHL-a mean (mg m^{-3})	Temperature range($^{\circ}\text{C}$)	Length after one year \pm SD (cm)	Reference
Maliakos Gulf	0.72	0.87-5.59	1.80	12.0-26.0	7.06 ± 0.46	Hatzonikolakis et al., 2017
Thermaikos Gulf	0.56	1.04-2.76	1.89	11.5-24.5	7.0 ± 0.47	Hatzonikolakis et al., 2017
Black Sea	Calibrated: 0.96	0.53-16.30	3.07	6.5-25.0	7.5 ± 0.1	Karayucel et al., 2010
Bizerte lagoon	3.829	4.00-7.70	5.20	12.0-28.0	7.26 ± 0.46	Béjaoui-Omri et al., 2014

1286

1287 Table 4. Half saturation tuned values (X_k) and mussel growth data (Length) in different areas of the Mediterranean and
 1288 Black Seas.

1289

1290

1291

Northern Ionian Sea			North Sea		
Variable	Value		Variable	Value	
Start date	20 Nov 2010		Start date	1 Jul 2014	
L	0.85 cm		L	0.15 cm	
W	0.1938 g		W	0.0055 g	
V	0.0096 cm^3		V	$5.3 \cdot 10^{-5} \text{ cm}^3$	
E	350 J		E	10 J	
R	0 J		R	0 J	
C	0 particles individual ⁻¹		C	0 particles individual ⁻¹	

1302 Table 5. Dynamic energy budget-accumulation model: initial values. L: shell length; W: fresh tissue mass; V: structural
 1303 volume; E: energy reserves; R: energy allocated to reproduction; C: Microplastics accumulation

1304

1305

1306

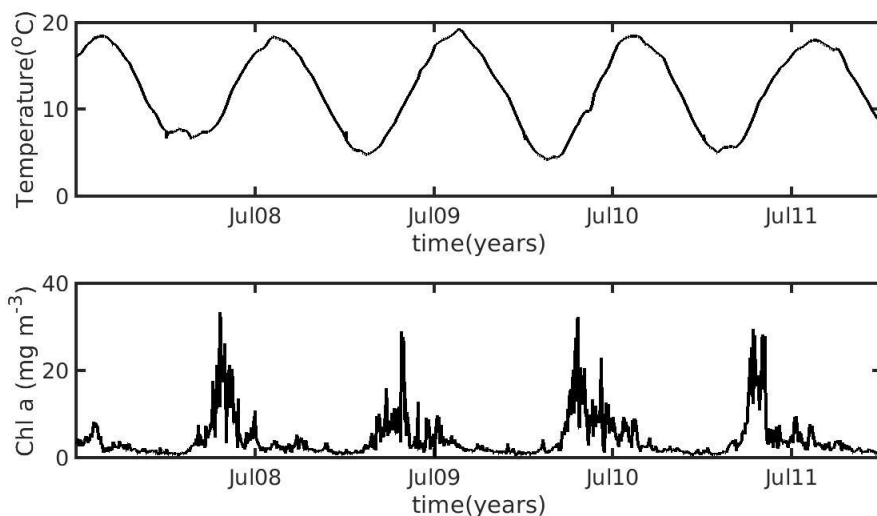


Fig. 1. Environmental data used for the forcing of the dynamic energy budget model in the North Sea simulation, showing temperature (top) and chlorophyll a concentration (bottom).

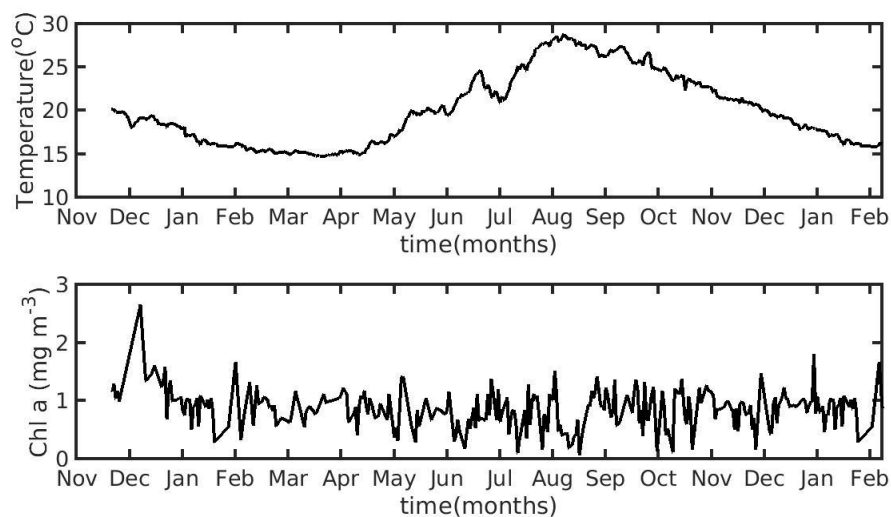
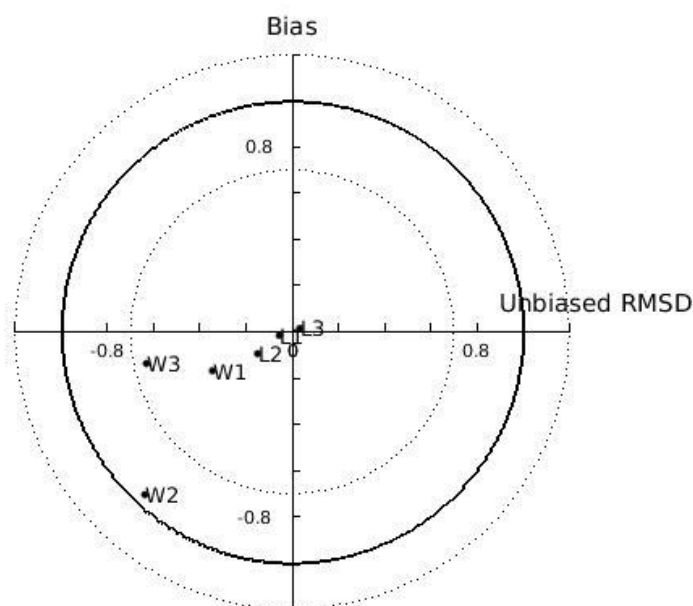


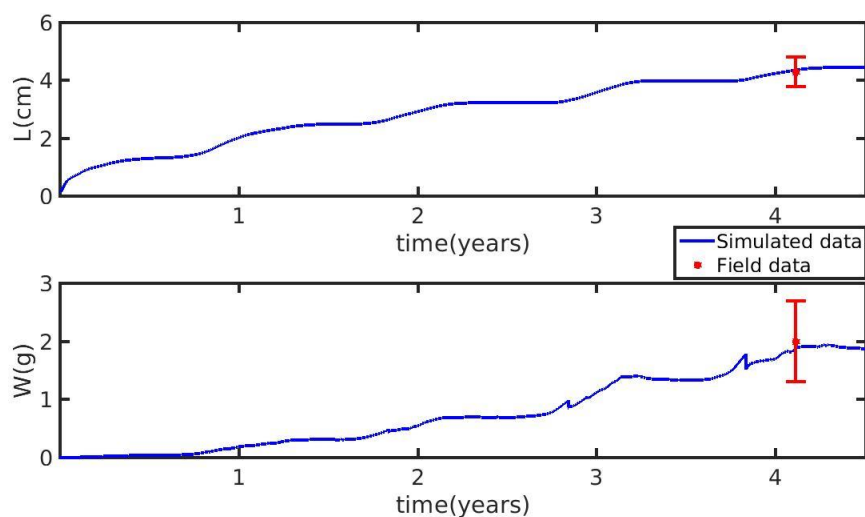
Fig. 2. Environmental data used for the forcing of the dynamic energy budget model in the Northern Ionian Sea simulation, showing temperature (top) and chlorophyll a concentration (bottom).



1318

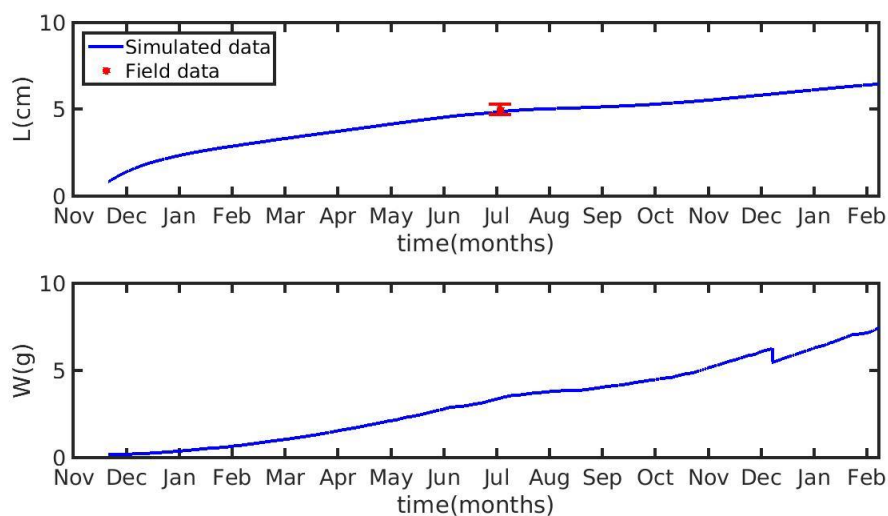
1319 *Fig. 3. Target diagram of simulated shell length (L) and fresh mass tissue weight (W) against field data from*
 1320 *Thermaikos and Maliakos Gulf (eastern Mediterranean Sea), Black Sea and Bizerte Lagoon (southwestern*
 1321 *Mediterranean Sea), using the **power** (L_1 , W_1), **exponential** (L_2 , W_2) and **linear** (L_3 , W_3) function of the half saturation*
 1322 *coefficient. The model bias is indicated on the y-axis while the unbiased root-mean-square-deviation (RMSD) is*
 1323 *indicated on the x-axis.*

1324



1325

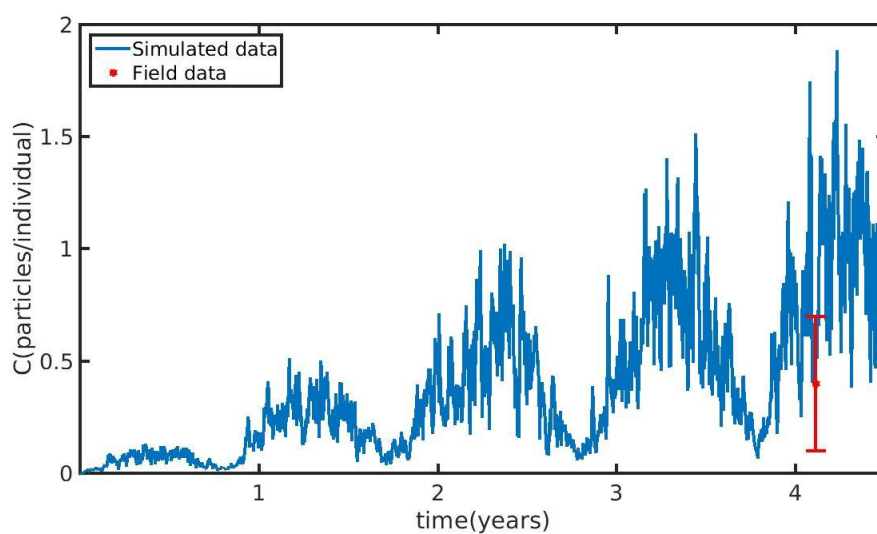
1326 *Fig. 4. Simulated mussel shell length (L) (top) and fresh tissue mass (W) (bottom) against North Sea data (red star:*
 1327 *mean \pm SD), using chlorophyll a ($X = [CHL-a]$) in the mussel diet.*



1328

1329 *Fig. 5. Simulated mussel shell length (L) (top) and fresh tissue mass (W) (bottom) against Northern Ionian Sea data*
 1330 *(red star: mean \pm SD), using chlorophyll a ($X = [CHL-a]$) in the mussel diet.*

1331



1332

1333 *Fig. 6. Microplastics (MPs) accumulation by the mussel (blue line) against field data (red star: mean \pm SD), using daily*
 1334 *environmental concentration of MPs (C_{env} mean value \pm SD: 0.4 ± 0.3 particles L^{-1}) in the North Sea.*

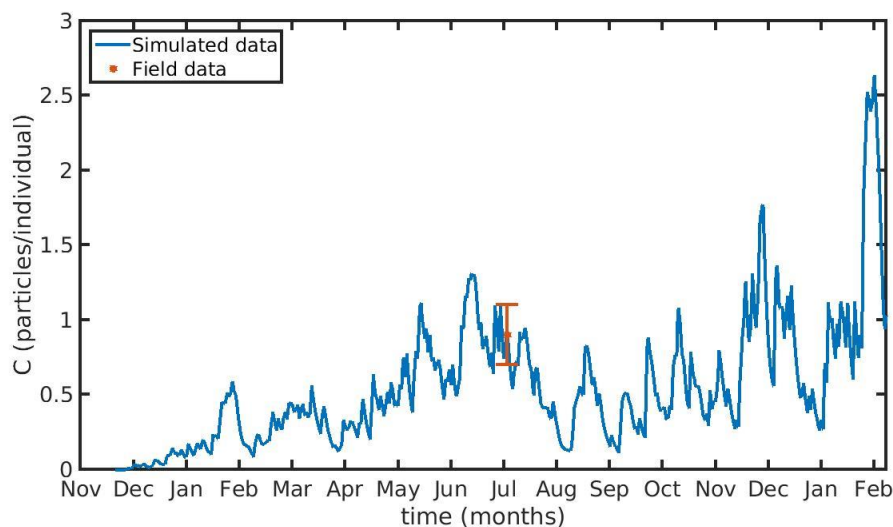


Fig. 7. Microplastics (MPs) accumulation by the mussel (blue line) against field data (red star: mean value \pm SD), using daily environmental concentration of MPs (C_{env} mean value \pm SD: 0.0012 ± 0.024 particles L^{-1}) in the Northern Ionian Sea.

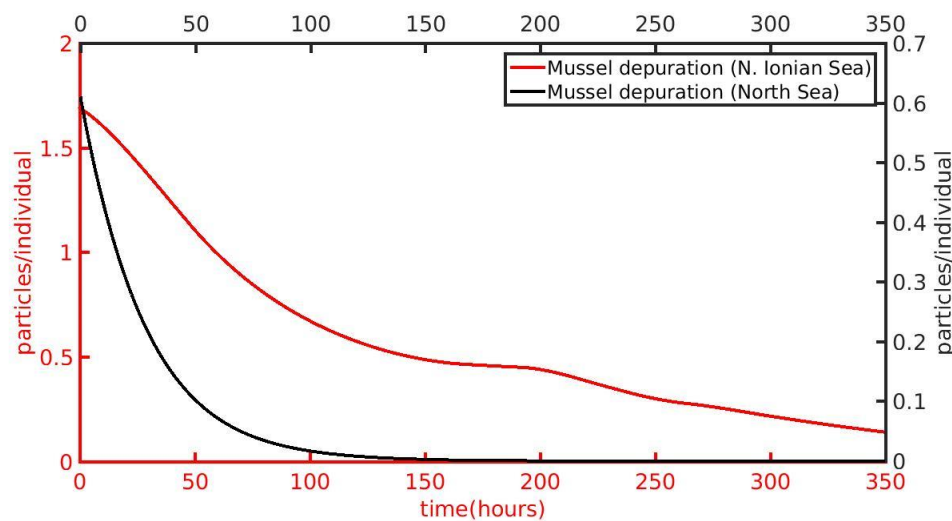
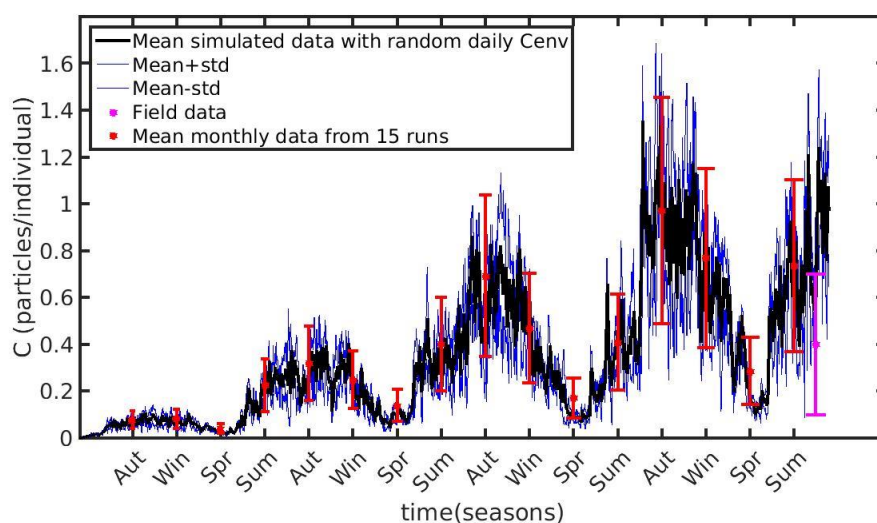


Fig. 8. Depuration phase of the cultured *Mytilus galloprovincialis* (red line) and wild *Mytilus edulis* (black line) using zero environmental concentration of microplastics ($C_{env}=0$) after 1 year and 4 years of simulation time at the Northern Ionian Sea and North Sea respectively.





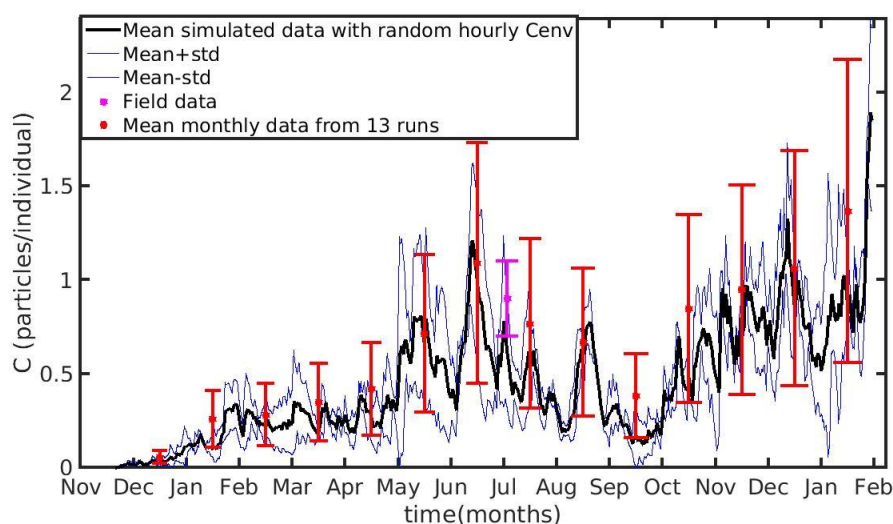
1347



1348

1349 *Fig. 9. Mean seasonally values and standard deviation of microplastics (MPs) accumulation (red error bars: mean*
 1350 *value \pm SD) by the mussel in North Sea derived from 15 model runs with different constant values of environmental*
 1351 *MPs concentration (C_{env} range: 0.1-0.8 particles L^{-1}); Mean hourly simulated data (black line) and standard deviation*
 1352 *(blue lines) of microplastics accumulation derived from 3 model runs with stochastic sequences of daily random C_{env}*
 1353 *values.*

1354



1355

1356 *Fig. 10. Mean monthly values and standard deviation of microplastics accumulation (red error bars: mean*
 1357 *value \pm SD) by the mussel in Northern Ionian Sea derived from 13 model runs with different constant values of environmental*
 1358 *MPs concentration (C_{env} range: 0.0012-0.024 particles L^{-1}); Mean hourly simulated data (black line) and standard deviation*
 1359 *(blue lines) of microplastics accumulation derived from 3 model runs with stochastic sequences of daily random C_{env}*
 1360 *values.*

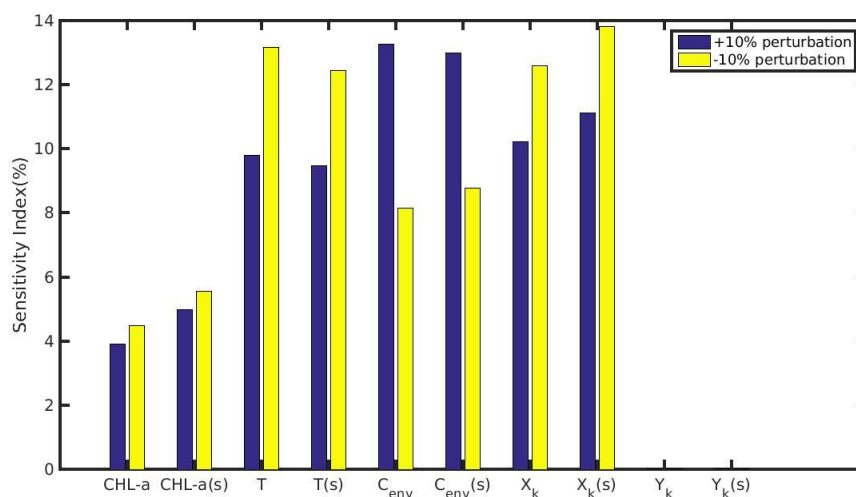


Fig. 11. Sensitivity index of MPs accumulation on the wild mussel of the North Sea when variables (CHL-a, temperature, C_{env}) and parameters (X_k, Y_k) are perturbed $\pm 10\%$. The notation (s) refers to the permanently submerged mussel.

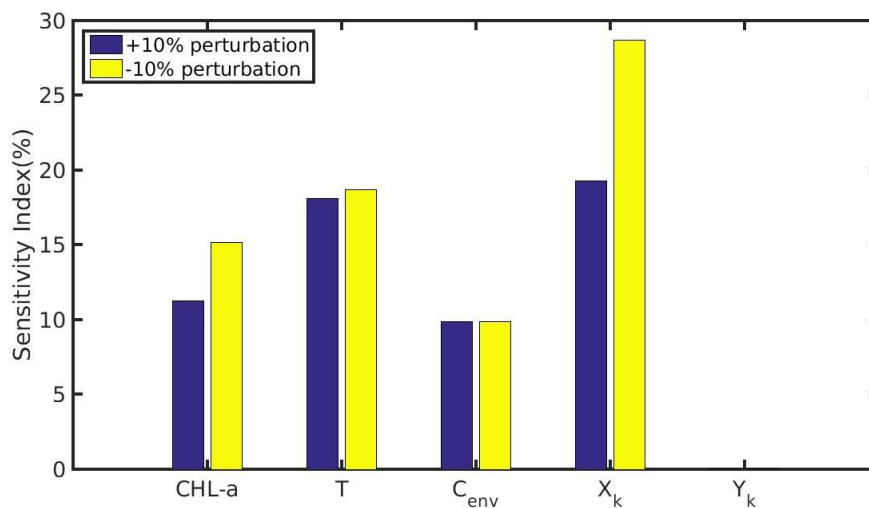


Fig. 12. Sensitivity index of MPs accumulation on the cultured mussel of the Northern Ionian Sea when variables (CHL-a, temperature, C_{env}) and parameters (X_k, Y_k) are perturbed $\pm 10\%$.

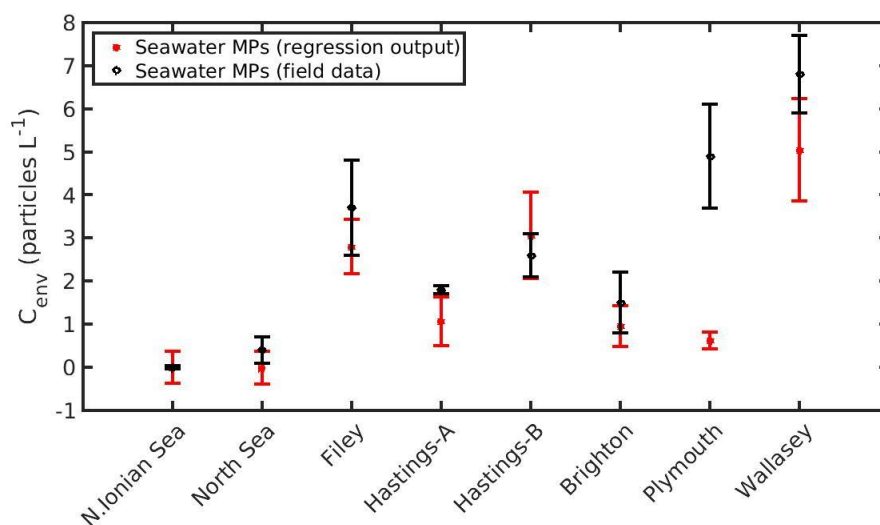


Fig. 13. Prediction of seawater microplastics concentration by using Eq. 20 for the Northern Ionian Sea, North Sea (present study) and 6 areas around U.K. (Filey, Hastings-A&B, Brighton, Plymouth, Wallasey; Li et al. (2018)).